UCRL-10496

University of California

Ernest O. Lawrence Radiation Laboratory

TWO-WEEK LOAN COPY

This is a Library Circulating Copy which may be borrowed for two weeks. For a personal retention copy, call Tech. Info. Division, Ext. 5545

EJECTION OF LARGE FRAGMENTS IN HIGH ENERGY NUCLEAR REACTIONS

Berkeley, California

DISCLAIMER

This document was prepared as an account of work sponsored by the United States Government. While this document is believed to contain correct information, neither the United States Government nor any agency thereof, nor the Regents of the University of California, nor any of their employees, makes any warranty, express or implied, or assumes any legal responsibility for the accuracy, completeness, or usefulness of any information, apparatus, product, or process disclosed, or represents that its use would not infringe privately owned rights. Reference herein to any specific commercial product, process, or service by its trade name, trademark, manufacturer, or otherwise, does not necessarily constitute or imply its endorsement, recommendation, or favoring by the United States Government or any agency thereof, or the Regents of the University of California. The views and opinions of authors expressed herein do not necessarily state or reflect those of the United States Government or any agency thereof or the Regents of the University of California.

Phys. Rev.

UCRL-10496

UNIVERSITY OF CALIFORNIA
Lawrence Radiation Laboratory
Berkeley, California

Contract No. W-7405-eng-48

EJECTION OF LARGE FRAGMENTS IN HIGH ENERGY NUCLEAR REACTIONS

Vitor P. Crespo, John M. Alexander, and Earl K. Hyde

October 1962

EJECTION OF LARGE FRAGMENTS IN HIGH ENERGY NUCLEAR REACTIONS

Vitor P. Crespo, John M. Alexander and Earl K. Hyde

Lawrence Radiation Laboratory
University of California
Berkeley, California

October 1962

ABSTRACT

The formation cross section for Na^{24} and Mg^{28} was measured in targets of Cu, Ag, Au, and U bombarded with protons and helium ions over the energy range 300-880 MeV. In addition the kinetic energy of these products was measured by a thick-target, catcher-foil technique. In the case of the proton bombardments the results were compared to the predictions of the conventional model of high energy regions i.e. a fast nucleonic cascade followed by a slower deexcitation cascade. It is found that the conventional model cannot even roughly reproduce the results and hence that another reaction mechanism, fragmentation, is required. Other evidence from radiochemical or emulsion studies of fragment production is reviewed and those features requiring explanation are emphasized. Possible views of a fragmentation mechanism are presented. A great similarity is found between the helium-ion-induced and the proton-induced results. This surprizing fact is taken as evidence that meson production and reabsorption processes are not the dominating feature of fragmentation reactions.

EJECTION OF LARGE FRAGMENTS IN HIGH ENERGY NUCLEAR REACTIONS*

Vitor P. Crespo†, John M. Alexander, and Earl K. Hyde

Lawrence Radiation Laboratory
University of California
Berkeley, California

October 1962

I. INTRODUCTION

This paper describes a radiochemical study of the production characteristics of the radionuclides Na^{24} and Mg^{28} in targets of copper, silver, gold, and uranium bombarded with 700 MeV protons and with helium ions in the energy range of 300-880 MeV. The formation cross sections were measured by standard techniques. In addition, certain recoil properties of these products were measured by a thick-target technique. These recoil experiments provided a measure of the intrinsic kinetic energy of the products and of the center-of-mass velocity of the heavy progenitor of the Na^{24} and Mg^{28}. The experimental quantities were compared with the predictions of various reaction mechanisms. The purpose of the investigation was to provide information on the mechanism of fragmentation, a fast violent process, in which a complex nucleus is divided into two or more complex aggregates of nucleons. Since the results have meaning chiefly when discussed in the context of previous studies of the interaction of high energy particles with complex nuclei, we begin by reviewing certain features and conclusions of previous studies.

A commonly-used description of high energy reactions is a two stage mechanism consisting of a fast cascade step followed by a slow evaporation

step. In the first stage the incoming particle undergoes an elastic or inelastic collision with an individaul nucleon in the nucleus. This collision may initiate a complex cascade during which a few high energy nucleons escape from the nucleus and large amounts of energy are absorbed by the target nucleus. It is also possible that the bombarding particle escapes after only a single collision carrying off most of its original energy. In the general case a wide distribution of excitation energy is left in the collection of struck nuclei. In the second step the excitation energy of the struck nuclei is dissipated by successive evaporation of several neutrons, protons, and alpha particles. With lesser probability there may be evaporation of heavier aggregates of nucleons. In the case of the heavier elements deexcitation may also occur by nuclear fission.

This two-step model predicts only four categories of reaction products: (1) Prompt-Cascade Neutrons and Protons emitted with a broad spectrum of kinetic energies ranging up to full energy of the bombarding particle. It is possible that alpha particles or more complex aggregates of nucleons existing as a transient sub-structure in the nucleus may participate in the high energy cascade and be ejected from the nucleus. (2) Evaporated Nucleons or Nucleon Aggregates emitted symmetrically in the center of mass system with an energy distribution characterized by a Coulombic barrier and a nuclear temperature. Neutrons, protons, and helium ions are most prominent but some contribution may be expected from fragments of higher Z; these contributions may be expected to decrease strongly as the charge of the fragment increases. (3) Fission Products and (4) Evaporation Residues. These last are the stable or radioactive nuclides remaining at the end of the evaporation chain.

The detailed characteristics of the high energy cascade have been calculated by Monte Carlo techniques for a representative group of target

elements and bombarding particle energies.[1-5] The most extensive calculations are those of Metropolis et al.[5] which covered two energy ranges — (1) bombarding energies for which only elastic collisions were significant and (2) bombarding energies up to 2 GeV in which inelastic, meson-producing, collisions are expected to occur in considerable frequency. Such calculations lead to predictions of cascade particle frequency, angular distribution, and energy distribution which can be compared with data obtained in nuclear emulsion studies of proton and alpha particle tracks. When the energy of the bombarding particle is insufficient for significant meson production the agreement of the emulsion data with the calculations is quite close. In the higher energy ranges the agreement is only fair owing probably to errors in the input data on inelastic collisions for the Monte Carlo calculations.

The calculations of the cascade step also lead to a prediction of a set of excited nuclei and a distribution in excitation energy for those nuclei. These predictions cannot be used for a direct comparison with experimental data but they may be used as the input data for a calculation of evaporative deexcitation. Such calculations[4,6,7,8] lead to a prediction of frequency and energy spectra of light evaporated particles, chiefly neutrons, protons, and alpha particles, which can be compared with the black prong data of nuclear emulsion studies. The calculations also lead to a prediction of the yields of heavy residual nuclei which can be compared to experimental cross section data obtained by radiochemistry and mass spectrometry.

Miller and Hudis[9] have thoroughly reviewed the fast-cascade-plus-evaporative-deexcitation mechanism of high energy reactions, published Monte-Carlo calculations of the two stages of the reaction, and the confrontation of the predictions with results obtained in emulsion and radiochemical

experiments. In general it has been concluded that there is good-to-excellent agreement of many of the experimental results with the predictions of the model for bombarding energies up to several hundreds of MeV. In the GeV energy range there is only fair agreement although much better agreement might be expected if better input parameters for inelastic collisions are found and used in a revised calculation.

We are not concerned here with a detailed examination of those features of high energy reactions which seem explained or capable of explanation by the conventional description of the reaction mechanism. We wish instead to call attention to a growing body of phenomena which cannot be described adequately by the model and which suggest the necessity to extend its scope or to consider the existence of an additional reaction mechanism fundamentally different in nature.

The term fragmentation has been applied to this different mechanism or mechanisms. We shall describe below some of the various meanings which have been attached to it. At this point we state only that fragmentation is some violent fast disruption of the nucleus which leads to the production of complex aggregates of nucleons in much greater yield than can be explained by the cascade-evaporation mechanism. Fragmentation may be a fission-like-process in that two or more chunks of the nucleus may separate and achieve considerable kinetic energy by mutual Coulombic repulsion, but it differs from fission in speed, and in the angular, energy, and mass distributions of the products.

A. Emulsion Evidence for Fragmentation

Much of the information suggesting a fragmentation process has come from nuclear emulsion studies in which light fragments with charge greater than 2 have been identified. This information is collected in an excellent

review article by Perfilov, Lozhkin and Shamov.[10] A number of the more significant articles are cited below.[11-22]

The majority of the emulsion data pertain to the production characteristics of Li^8 because of the easily-identified "hammer tracks" resulting from the decay of Li^8 into Be^8 which instantly disintegrates into two alpha particles. However, there are some data, particularly in the Russian literature,[10,-13a] in which tracks of fragments with $Z > 3$ have been studied.

The frequency of occurrence of these light fragments is a steep function of bombarding energy in the range 100 MeV to several GeV and the stars associated with fragment production contain a substantially larger number of cascade proton tracks than do the average of all stars. These facts indicate that fragment production is favored by very high energy transfers in the cascade step. The energy spectrum of these light fragments has the general appearance of an evaporation spectrum but it is in most cases too broad to be explained by any reasonable choice of evaporation parameters.[14-18] In addition, several authors have reported a group of high energy fragments many tens of MeV beyond the maximum of the evaporation spectrum.[7,17,19] In some cases energies greater than 100 MeV have been found.[13,18] These higher energy fragments have special characteristics. For example, Nakagawa, Tamai, and Nomoto[17] reported that the yields of the highest energy group of Li^8 fragments produced in the bombardment of emulsion with 6 GeV protons had a strong dependence on the number of cascade charged particles (grey tracks) but no dependence on the number of evaporated charged particles (black prongs) emitted from the same star. This suggested strongly that these Li^8 fragments were not evaporated but were produced somehow in the cascade process. A similar result was reported by Goldsack, Lock, and Murin.[20] These authors also pointed out that a lower energy group of Li^8 fragments occurring in complex stars with more than 12 black prongs had an

isotropic distribution with respect to the bombarding protons, whereas a higher energy group associated with less complex stars was peaked strongly forward.

Katcoff[15] placed foils of Cu, Ag, Au, and U in a beam of 2.2 GeV protons and examined the properties of Li^8 fragments ejected from the targets and caught in nuclear emulsions. The energy spectrum in the case of the silver target was approximately correct for an evaporation spectrum but in the other three cases it was too broad and had too much intensity in the higher energy regions.

In the examination of stars in nuclear emulsions it is sometimes observed that two or more fragments with $Z > 2$ are emitted in a single nuclear disintegration.[10,11,16] From evaporation theory such events should have an exceedingly low probability but experimentally it is found that in several percent of the events containing any fragments whatsoever there is double or triple fragment emission.

The evaporation model would predict a moderate favoring of emission in the forward direction with respect to the beam because of a small center-of-mass motion of the struck nucleus. Many authors found a more pronounced favoring of the forward hemisphere than seemed reasonable[11,14] although Skjeggestad and Sörensen[13] concluded that the forward peaking of Li^8 fragments could be accounted for satisfactorily. Some like Baker and Katcoff[19] (emulsion plus 1, 2, and 3 GeV protons) and Perkins[16] (emulsions plus cosmic rays) have noted a preference for sideways emission with respect to the beam in addition to the expected forward peaking.

Some authors have reported favored directions of emission of fragments with respect to the tracks of alpha particles, protons, residual heavy nuclei and other fragments, which suggest that the fragment and the entity making the

correlated track are emitted simultaneously.

Several authors have considered and rejected[11,14,17,18] the hypothesis that Li^8 and other light fragments are produced by a direct elastic collision of the incoming particle with a Li^8 or similar sub-group in the nucleus. Such a model is not compatible with the observed lack of correlation of the energy of the fragment and the angle of emission. Nor can it account for multiple fragment emission and other features.

The overall conclusion from these emulsion studies is the following. Although the conventional reaction mechanism of cascade plus evaporation undoubtedly explains the formation of part, perhaps in many cases the major part, of the light fragments, there is a strong evidence for the existence of an additional process for their formation.

B. Radiochemical Evidence for Fragmentation

Let us now consider the radiochemical evidence which consists chiefly of the formation cross section and excitation functions for several radioactive nuclides in the mass range 7 to ~ 40 produced in various target elements bombarded with high energy particles. Some of the nuclides studied—such as He^6, Be^7, C^{11}, N^{13}, and F^{18}— overlap the range of mass numbers covered in the emulsion studies. Others—such as Na^{22}, Na^{24}, Mg^{28}, Si^{31}, P^{32}, and P^{33}— are considerably heavier in mass. The excitation functions for such products show a sharp rise starting about 200 MeV and continuing to about 2 GeV[23,24,25], above which there is a sharp leveling off in cross section.

Several authors[25,26] have noted an interesting variation in the cross sections of such products as F^{18}, Na^{24} and P^{32} as a function of the target mass number when the energy of the bombarding particle is fixed at some value above a few hundred MeV. Later on we shall discuss our own results bearing on

this point in connection with Figs. 5 and 6 below. Up to a target mass number of $\approx$ 150 there is a decrease in cross section whereas above mass 180 there is a marked increase. It seems difficult to explain the yield increase for the higher mass targets by a spallation mechanism, and Caretto, Hudis, and Friedlander[25] attributed it to fragmentation.

The cross section versus mass number curves for products formed in heavy target elements by GeV proton reactions also have a peculiar form which has been cited as evidence for a fragmentation mechanism. Wolfgang et al.[24,24a] studied the interaction of lead with protons of 1.0 to 3.0 GeV energy. A rather remarkable feature of the total isobaric cross sections is their near constancy over the entire range of masses. From mass 20 up to the mass of the target the yields differ only by a factor of 10 or 20. This curve is entirely different from those determined for bismuth targets bombarded with 340 or 480 MeV protons. In the latter cases there is a prominent group of fission products and a clearly identifiable group of spallation products (evaporation residues) close in mass to the target mass. The yields of products in the latter group drop off rapidly as the product mass number decreases.

A consideration of the radiochemical data in the lead-bismuth targets led Wolfgang et al.[24] to postulate a fast fragmentation of the nucleus resulting from local heating caused by the production and reabsorption of pions.

C. Purpose and Scope of Present Work

The present work was undertaken in the belief that additional data on the formation properties of Na^{24} and Mg^{28} would confirm the need for the postulated fragmentation process and throw some light on its nature. Na^{24} and Mg^{28} were chosen because of their convenient radiochemical properties and because there seemed little reason to believe that they could be formed

in high yield either as evaporated particles or cascade-evaporation residues in targets as heavy as silver, gold, or uranium. In the case of copper targets it seemed likely that they would be produced chiefly as evaporation residues but it was deemed desirable to verify this. The existence of a considerable amount of Na^{24} cross section data for proton-induced reactions was also an advantage in the discussion of our results. Except for these features there is nothing special about Na^{24} and Mg^{28}; hence they may serve as representatives of the behavior of a whole class of products of roughly similar mass produced in high energy reactions.

In separate experiments the target elements were bombarded with 700 MeV protons, and with 320, 500, 700, and 880 MeV helium ions and the formation cross sections were measured by the radiochemical techniques given in detail below. The comparison of the helium-ion-induced production curves with those for proton-induced production was thought to be particularly significant in evaluating the contribution of meson effects to fragmentation yields. It was anticipated that helium ions of a given energy would be much less effective in creating mesons in the targets nuclei than protons of the same energy. Hence, if fragments such as Na^{24} are indeed produced exclusively by a mechanism involving production and reabsorption of mesons then the production cross section should be substantially less when helium ions are substituted for protons.

In addition to cross section measurements our experiments also included a study of the recoil properties of the fragments.

Our plan in the analysis of the cross section and recoil range results was to assume at first the correctness of the conventional two-stage description of high energy reactions. We then made a number of qualitative and quantitative comparisons of the predictions of this model with those characteristics which could be extracted from our experimental data under the

assumption that the model was correct. A major fraction of this paper consists of the development of this comparison. It will be found that there appears to be internal contradictions of fundamental importance when the data are treated in the framework of the conventional model particularly at the higher bombarding energies. We will conclude that the conventional view of a fast stage plus slow stage cannot account for the production of such nuclides as Na^{24} and Mg^{28} in targets of silver, gold, and uranium and may not account for it even in targets of copper. We then consider other possible methods for the production of such fragments.

II. CROSS SECTION DATA

A. Experimental

Target assemblies. The target assembly used in the determination of cross sections consisted of a stack of 1.5 x 2 cm foils arranged as shown in Fig. 1. The target foils designated T_1 T_2 T_3 and T_4 were separated from one another by 0.003 inch mylar foils (designated My). All cross sections were measured relative to Na^{24} produced in the aluminum monitor foil (Al-Mon). The number of target foils used in any particular experiment varied from one to four. The copper target foils were 0.002 inches thick; all others were 0.001 inches thick. Spectrochemical analysis of the target foils showed the following levels of contamination: copper targets - 0.03% Al; silver targets - 0.1% Cu and 0.02% Al; gold targets - 0.3% Cu; uranium targets - 100 ppm of Si and 10 ppm of Cu Co and Mg; Aluminium targets - 0.05% of Cu and Fe. It was of critical importance to align exactly the different foils in the stack because most of the beam struck the leading edge. To insure proper alignment the leading edge was machined after the stack was fastened to the target holder. The stack was then wrapped in 0.001 inch thick mylar film.

All foils were cleaned before mounting for irradiation. Copper and gold foils were cleaned with dilute nitric acid; uranium foils with 2 to 6M nitric acid and silver foils with ammonia. All foils were then washed with acetone and rinsed with distilled water.

Irradiations and beam monitoring. The irradiations were performed at the 184" cyclotron and the bevatron. Bombardment times varied from 1 to 1.5 hours.

The Na^{24} produced in the aluminum monitor foils by the reaction Al^{27} (p,3 pn) or $Al^{27}(\alpha,\alpha\ 2pn)$ was determined by cutting up the monitor foils and mounting them in a fashion to reproduce as closely as possible the conditions used for activity measurements in the samples isolated radiochemically from the target. The monitor cross sections were taken as 10.7 mb for Al^{27}(p,3 pn) Na^{24} and as 24.0 mb for $Al^{27}(\alpha,\alpha\ 2pn)$ Na^{24} for all energies. The proton-induced cross section has been determined over a wide range of energy[27] but the value of 24.0 mb bombardment for the alpha-induced reaction is that measured at the single energy of 380 MeV.[28,29] The cross section is not expected to change drastically between 380 and 880 MeV, but an uncertain error is associated with the monitor cross section and with the cross section reported below in targets bombarded with the higher-energy helium ions.

Treatment of targets after bombardment. After bombardment the metal foils were dissolved in an appropriate acid in the presence of a few milligrams of sodium and magnesium carrier. By means of the radiochemical procedure outlined in the Appendix, sodium and magnesium fractions were recovered from the solution in a high state of radiochemical purity. In the final step of the magnesium procedure an 8-hydroxyquinoline compound was precipitated, filtered, dried, and weighed to determine the percentage chemical recovery. Similarly in the final step of the sodium procedure sodium chloride was

precipitated from a solution of butanol saturated with hydrochloric acid.

The activity of the Na^{24} and Mg^{28} samples was measured in end-window proportional counters over a period of days. The 15 hour decay of Na^{24} could easily be resolved from the almost negligible background in the sodium fractions. The 21 hour decay of Mg^{28} was easy to resolve from the magnesium samples but there was some contamination of the samples by longer-lived activities. Activity measurement techniques and corrections are discussed in the Appendix.

B. Results and Discussion

Cross section results for the different targets and bombarding particles are listed in Table I. The ratio of the cross sections $\sigma_{Mg^{28}}/\sigma_{Na^{24}}$ is also tabulated. The number of determinations of any particular cross section is given in parentheses after the cross section values. The numbers given are average values and the errors quoted are the standard errors.

The Na^{24} and Mg^{28} cross sections are plotted in Figs. 2 and 3 versus alpha particle bombarding energy for the different targets. Figure 4 is a similar plot of Na^{24} cross sections from proton bombardments; most of the points on this plot are taken from data in the literature. The principal feature we note on all three figures is that the probability of formation remains low for all targets until the bombarding energy reaches some hundreds of MeV. Then it increases rapidly but levels off again in the GeV range of energies. Similar results have been observed for other fragments[22-26, 37] (Be^7, F^{18}, P^{32}, P^{33} and others).

At a given energy of the bombarding particle the yields of Na^{24} and Mg^{28} are higher by a factor of two when helium ions are substituted for protons as the bombarding particle. Table II summarizes numerical values for

700 MeV particles. This observation is subject to the large uncertainty in the monitor reaction cross section for 700 MeV helium ions, but it is not likely that this cross section is off by a factor of 2. Hence, we have the unexpected result that helium ions are as effective as protons in causing fragmentation of the nucleus. The values of $\sigma_{Na}^{24} / \sigma_{Mg}^{28}$ are larger for the heavier targets (Au - U) than for the lighter ones (Cu - Ag) and are within experimental error independent of the bombarding energy.

The results are replotted in Figs. 5 and 6 to show the variation of cross section with the mass of the target. The turn-up of the yield at the higher target masses, which was observed earlier in the case of proton bombardments by Caretto, Hudis, and Friedlander[25] is seen to occur also for helium-induced reactions.

The overall similarity of such characteristics as threshold values, shapes of the excitation function, and yield variation with target mass number, whether helium ions or protons are used, suggests strongly that the helium ions and the protons generate a cascade in the nucleus of very similar character and that the helium ion acts as a single particle and not as a collection of 2 neutrons and 2 protons interacting individually with the target nucleons.

In the framework of the conventional 2-stage reaction model the high threshold for the production of Na^{24} and Mg^{28} and the steady rise of the cross-section up to the GeV range of energies means that only those cascades which deposit greater than 250 MeV of energy are effective in producing Na^{24} and Mg^{28}. It means also that those cascades which deposit substantially more than 250 MeV are most effective in producing these nuclides.

Porile and Sugarman[38] have analyzed cross section results in a more formal way by writing down the expression.

$$\sigma_A (E_B) = \int_0^{E^*_{max}} \sigma_g \, N(E^*, E_B) \, F_A(E^*) \, d E^*$$

where the symbols have the following meaning.

$\sigma_A(E_B)$ is the cross section for the production of a product A when the energy of the bombarding particle is E_B.

σ_g is the total reaction cross section.

$N(E^*, E_B)$ is the fraction of nuclei left with an excitation energy E^* at the end of the fast cascade when the bombarding energy is E_B.

$F_A(E^*)$ is the fraction of the nuclei, excited to E^* at the end of the fast cascade, which deexcite in such a way as to form final product A. It is important to reemphasize at this point that the model under discussion assumes that the excitation energy and the charge and mass number of the nucleus at the end of the prompt cascade completely determine the spectrum of final products. The F_A function may be expected to be zero below some threshold then rise to a maximum value, and, finally, perhaps turn over and decrease at higher values of E^*.

To get some notion of the shape of the $N(E^*, E_B)$ function we can examine the results of the Monte-Carlo cascade calculations of Metropolis et al.[5] In Fig. 7 we sketch in the distribution found by these authors for the case of cerium bombarded with 238 and 368 MeV protons. We note that there is a very broad energy distribution in the struck nuclei from zero energy up to the energy of the bombarding particles. The only part of this distribution which is effective in the production of such nuclides as Na^{24} is the high energy tail. When the bombarding energy is raised, the curve in the region of high excitation rises and is extended to higher energies.

Because the energy distribution of the residual nuclei at the end of the prompt cascade is shifted only slowly with bombarding energy, and because the excitation function for the measured products rises rapidly with E_B above

a very high threshold, it follows that the $F_A(E^*)$ function is rapidly rising with E^* and that it is only those few cascades which lead to the highest values of E^* which are contributing the main part to the Na^{24} and Mg^{28} cross sections.

If one calculates or assumes an $N(E^*, E_B)$ distribution and a total reaction cross-section one can work backward from the experimental value of the Na^{24} or Mg^{28} production excitation functions to determine a branching ratio function, $F_A(E^*)$. Once the values of N and F have been fixed it is possible to calculate the average excitation energy, $\overline{E}$, of struck nuclei, which ultimately disintegrate to produce a product of mass A, by the following expression

$$\overline{E} = \int_0^{E^*_{max}} \sigma_g \; E^* \; N(E^*,E_B) \; F_A(E^*) \; dE \Big/ \int_0^{E^*_{max}} \sigma_g \; N(E^*,E_B) f_A(E^* dE^*)$$

We have carried through such an analysis for our results and conclude that for any reasonable form of $N(E^*, E_B)$ which is non-vanishing up to the bombarding energy, the average excitation energy for the production of Na^{24} in targets of copper, silver, gold, and uranium bombarded with 700 protons lies between 500 and 700 MeV in all cases. In the case of bombarding energies of 3 GeV the required average excitation energies are even higher.

This result in itself puts severe strain on the basic assumptions of the conventional reaction model as it is not all clear that nuclei excited to such huge energies can exist long enough to undergo deexcitation in a way adequately described by a statistical model of evaporation of small particles or clusters. In the case of copper targets these excitation energies are equivalent to the total binding energy in the nucleus.

It is possible to deduce that the $F(E^*)$ curves for the 4 target elements are very similar to each other by the following line of reasoning.

First of all we note that the published $N(E^*, E_B)$ spectra of Metropolis et al.[5] have nearly the same shape for all target elements <u>for the deposition energy region above 250 MeV</u> except for a proportionality constant. (See for example Fig. 15 in Ref. 5)

$$\text{i.e. } N(E^*, E_B)_{\text{Target 1}} = k\, N(E^*, E_B)_{\text{Target 2}}$$

Secondly we note from Fig. 4 that the excitation functions for the production of Na^{24} in targets of silver, gold, and uranium bombarded with proton are similar; the excitation function in the case of copper targets rises faster with bombarding energy up to 3 GeV and at higher energies stays more nearly constant than the corresponding excitation functions for silver, gold, and uranium. If the assumption is correct that the $N(E^*, E_B)$ distributions for large E^* differ only by a multiplicative constant then one expects the functions $F_A(E^*)$ for Na^{24} production from silver, gold, and uranium also to differ only by a constant factor and the function $F_A(E^*)$ for Na^{24} production in copper targets to be displaced toward lower energies in relation to the $F_A(E^*)$ functions for the other targets. We shall see below that these conclusions are inconsistent with those derived from the recoil range results if we try to explain all results by the assumed 2-stage mechanism.

III. RECOIL MEASUREMENTS

A. Basic Assumptions

Because of limitations imposed by beam intensities, low cross section values, and permissible target thicknesses it proved most convenient to use a very simple, integral-range technique originated by Sugarman et al.[38,39] for our measurements of recoil properties. In this method a thick target of precisely measured thickness is sandwiched between two mylar catcher foils whose thickness is greater than the range of the products being measured.

The recoil target assembly is shown in Fig. 8. The target foil (T) had dimensions 1.5 x 2 centimeters while the other foils had dimensions 1.9 x 2.2 cm. The Mylar foils (My) were 0.003 inch thick (much thicker than the recoil range of Na^{24} or Mg^{28}). Blank foils were included to serve as a measure of the production of Na^{24} and Mg^{28} due to activation of impurities in the mylar.

After the irradiation of this foil stack a radiochemical analysis was made to determine the amount of Na^{24} and Mg^{28} present in the target and in the upstream and downstream catcher foils. The radiochemical procedures, the methods of determination of radioactivity in the samples, and the corrections to the data are discussed in the Appendix.

From the corrected decay-rate data it was possible to compute the fractions of the total Na^{24} or Mg^{28} activity which remains in the target foil, and which recoils into the upstream and downstream catchers. These fractions are designated F_T, F_B, and F_F, respectively. Some foil stacks were also exposed at 10 deg to the beam, and in these experiments the fractions activity left in the target and that recoiling in a perpendicular direction into the two side foils were determined. These fractions are designated F_{TP}, F_{PB}, and F_{PF} respectively. The F (for forward) and B (for backward) in the latter subscripts allow for the fact that the bombardment stack is not precisely parallel to the beam. If the foil stack were precisely parallel F_{PF} and F_{PB} would be equal. The perpendicular recoil fraction was taken as $F_P = (F_{PF} + F_{PB})/2$.

The analysis of the recoil results in terms of the conventional two-step mechanism depends upon the following very general assumptions (a) the bombarding particle imparts to the target nucleus a velocity, $\underset{\sim}{v}$, which has a laboratory system component, $v_{\parallel}$, along the beam direction and a component, $v_{\perp}$, in a direction perpendicular to the beam. (b) when this struck nucleus disintegrates to form Na^{24} or Mg^{28} the break-up process provides

an additional velocity component $\underset{\sim}{V}$. This velocity $\underset{\sim}{V}$ reflects the intrinsic kinetic energy of the fragment in the frame of reference of the moving nucleus. (c) the range $\underset{\sim}{R}$ of the fragments, is proportional to the vector sum of $\underset{\sim}{V}$ and $\underset{\sim}{v}$. (d) the range is given by $\underset{\sim}{R} = k\,(|\underset{\sim}{V} + \underset{\sim}{v}|)^N$ where k and N are constants to be evaluated empirically from range energy data on fragments of similar size, charge and energy. (e) the angular distribution $W(\theta)$ of $\underset{\sim}{V}$ in the moving frame is given by

$$W(\theta) = a + b \cos^2 \theta$$

(f) the magnitudes of $\underset{\sim}{v}$ and $\underset{\sim}{V}$ are unique and (g) the path of the fragment is a straight line. (A more precise statement of assumption (g) is that the scattering of the observed fragments is similar to that of the energetic fragments of known energy which were used to calibrate the range energy curve.)

N. Sugarman[40] and L. Winsberg[41] have derived the necessary equations for the analysis of these experiments with the above assumptions. We use the notation $R_o = k\,V^N$, $\eta_{\parallel} \equiv v_{\parallel}/V$ and $\eta_{\perp} \equiv v_{\perp}/V$. If we neglect terms of order larger than $\eta_{\parallel}^2$, $\eta_{\perp}^2$ and $(b/a)^1$ we obtain the following set of equations.[40]

$$(1)\quad F_F = \frac{R_o}{4W}\left\{1 + \frac{1}{6}\frac{b}{a} + \eta_{\parallel}\left[2/3\,(N+2) + \frac{b}{a}\,8\,\frac{(N-1)}{45}\right] + \eta_{\parallel}^2\left[\frac{N+1)^2}{4} + \frac{b}{a}\,\frac{N^2-N-4}{12}\right] + \eta_{\perp}^2\left[\frac{N^2-1}{8} + \frac{b}{a}\,\frac{N-1}{12}\right]\right\},$$

$$(2)\quad F_B = \frac{R_o}{4W}\left\{1 + \frac{1}{6}\frac{b}{a} - \eta_{\parallel}\left[2/3\,(N+2) + \frac{b}{a}\,8\,\frac{(N-1)}{45}\right] + \eta_{\parallel}^2\left[\frac{(N+1)^2}{4} + \frac{b}{a}\,\frac{N^2-N-4}{12}\right] + \eta_{\perp}^2\left[\frac{N^2-1}{8} + \frac{b}{a}\,\frac{N-1}{12}\right]\right\}$$

and

$$(3)\quad F_P = \frac{R_{oP}}{4W}\left\{1 - \frac{1}{12}\frac{b}{a} + \eta_\perp^2 \frac{(N+1)}{16}\left((3N+1) + \frac{b}{a}\left(\frac{7-3N}{6}\right)\right) + \eta_\parallel^2 \frac{(N-1)}{8}\left((N+1) + \frac{b}{a}\left(\frac{N-5}{6}\right)\right)\right\}$$

Since there are four unknown quantities ($\eta_\parallel$, $\eta_\perp$, R_o and b/a) and only 3 equations it is necessary to introduce at least one additional assumption. We chose to proceed by assuming that $\eta_\perp = o$ and $b/a = 0$ and hence setting $\eta_\parallel = \eta$ and $v_\parallel = v$. These additional assumptions introduce only small errors in the calculated values of V and R_o and do not alter the conclusions. The effects of these assumptions are discussed in Appendix C.

In Appendix D we show that the value of N = 1.5 fits best in the equation, $R_o = k\ V^N$ for Na^{24} and Mg^{28} stopped in Cu, Ag, Au, and U. The proper values of the constant k are also given the Appendix D.

The working equations then reduce to

$$(4)\quad WF_F = \frac{R_o}{4}\left(1 + 2.333\ \eta + 1.562\ \eta^2\right)$$

$$(5)\quad W(F_F - F_B) = 1.166\ \eta\ R_o$$

$$(6)\quad WF_P = \frac{R_{oP}}{4}\left(1 + 0.156\ \eta^2\right)$$

B. Recoil Results

Tables III and IV contain the Na^{24} results and Tables V and VI the the Mg^{28} results. Table III and V contain the following information. Columns 1, 2, and 3 give the target, the number of determinations and the bombarding particles and their energy. Columns 4 and 5 list the products WF_F and WF_B needed for substitution in Eqs. 4 and 5. Columns 7 and 8 gives the quantities η and R_o derived from Eqs. 4 and 5. The range values

R_o are converted into energy values ($E = 1/2\ AV^2$) by use of the range energy expression $R_o = k\ V^{1.5}$ whose justification is discussed in the Appendix. These energy values are listed in Column 9.

The average velocity, $v_{||}$, imparted to the progenitor of the fragment is given by $v_{||} = \eta\sqrt{\frac{2E}{A}}$. This velocity is quoted in the tables and in Figs. 10 and 11 in units of $(\text{MeV/amu})^{1/2}$.

The measured and derived quantities from the perpendicular experiments are tabulated in Tables IV and VI.

C. Discussion of Recoil Results

We start our discussion of the recoil results with a consideration of the kinetic energy values (E) of Na^{24} and Mg^{28}. A glance at the tables indicates that the kinetic energy of these products is quite high, comparable indeed to the kinetic energy observed in heavy element fission products. As a measure of comparison we may compute the Coulombic energy which such a product might obtain by a fission-type division of the original nucleus into Na^{24} and its complementary fragment with atomic charge Z-11 and atomic number A-24, where Z and A are the atomic charge and number of the target nucleus. For the purpose of a crude estimate we simply compute the Coulombic repulsion of two tangent spheres with radii given by the expression $r = r_o A^{1/3}$ where r_o is taken as 1.45×10^{-13}cm.

The ratio of the experimentally measured recoil energy to this calculated $E_{Coul.}$ is a revealing quantity. If Na^{24} is in fact produced as the result of the evaporation of many smaller particles from an excited heavier nucleus then the ratio should be low, say < 0.5. A ratio approaching the value 1 would strongly suggest that the kinetic energy of the Na^{24} comes from the Coulombic repulsion of large fragments.

The values of $E/E_{Coul.}$ are given in Fig. 9. All values are approximately equal to 0.7 indicating that a fission-like division of the nucleus has probably occurred. The Coulombic energy has, to be sure, been estimated in a very approximate way but any correction to this quantity to allow for loss of cascade particles in advance of division of the nucleus, or for thermal expansion, or for shape deformations of the separating fragments will reduce the estimate of $E_{Coul.}$ and hence increase the ratio $E/E_{Coul.}$. The large values of this ratio suggest that even in copper targets and even at bombarding energies of 3 GeV Na^{24} and Mg^{28} are not produced by a cascade followed by the evaporation of many small particles, contrary to what one might have assumed. The similar values of $E/E_{Coul.}$ suggest that the same mechanism may be responsible for fragment production in all target nuclei. This is a surprising result since, as indicated earlier, the excitation function data as interpreted by the conventional model show that at the bombarding energies used in this work more than 500 MeV of excitation are required in order to have "fragmentation". Such deposition energies are large enough to allow production of Na from Cu as the residue of a cascade evaporation process. This is emphasized by the fact that the total binding energy of copper is approximately 570 and of silver is approximately 920 MeV. If any sizeable fraction of the disintegrations leading to Na^{24} production went by this evaporation mechanism the value of $E/E_{Coul.}$ should be smaller for Cu than for the other targets.

We turn now to a consideration of the values of v, defined as the velocity of the struck nucleus, and obtained from the recoil data with the aid of the Eqs. 4 and 5. Under the assumption that the progenitors of the fragments have mass values very nearly equal to the target mass, the average momenta, $\overline{P}_T = v_{\parallel} \times A_{target}$, imparted to the struck nuclei in the beam direction

have been calculated. These values are given in column 10 of Tables III and V. We have also computed the ratio $\overline{P}_T/P_{CN}$ where P_{CN} is the momentum of the hypothetical compound nucleus or equivalently, the momentum of the bombarding particle. These ratios are plotted in Figs. 10B and 11B for Na^{24} and Mg^{28} respectively. Because the progenitors of the fragments are expected to have somewhat less than the mass of the target nucleus when account is taken of the loss of particles in the initial cascade, $\overline{P}_T$ is a slight overestimate of the actual momentum transferred. It is to be noted that the values of $\overline{P}_T/P_{CN}$ are larger than 1 for 700 MeV protons and 880 MeV α incident on gold and uranium targets. This may be due to the overestimate of $\overline{P}_T$. It is also known that particular cascade events may result in struck nuclei with more forward momentum than is brought in by the bombarding particle if the internal motions of the target nucleons are considered. See for example Fig. 1 in an article by Porile.[42] For some unknown reason the process leading to Na^{24} production may select out these particular cascade events. A third explanation, which we favor in our remarks below, is that the observed fragments are not produced by the 2-stage process postulated in the conventional analysis so that the calculated quantities $v_{\parallel}$ and $\overline{P}_T$ do not have a real meaning.

For the present, however, we continue to explore the implications of our data within the framework of the conventional 2-stage mechanism to demonstrate a further major inconsistency. We call attention to the fact that the ratio, $\overline{P}_T/P_{CN}$, must have some relation to the ratio, E^*/E_{CN}; in general one would expect the forward component of momentum of the struck nucleus to increase as the amount of energy transferred to the struck nucleus increases. The quantitative interdependence of these quantities depends on the details of the model of the prompt cascade process. Porile[42] examined the detailed cascade calculations of Metropolis et al.[5] for targets of ruthenium, bismuth and

uranium bombarded with protons and was able to construct a plot, which we reproduce here as Fig. 12, showing the average deposited forward momentum as a function of the deposited energy, both expressed in units of the corresponding values for compound nucleus formation. It is seen that the deposited momentum increases almost linearly with increasing deposition energy, and as a first approximation, the relationship between P_F/P_{CN} and E^*/E_{CN} can be considered to be independent of the bombarding energy and target material. There would seem to be no reason why this should not be true also for the targets used in our study.

If we now reexamine our values of P_T^*/P_{CN} we note that there is a strong increase in this value with increase in target mass number which implies an increase in excitation energy, E^*, with increase in target mass number. But in our discussion above of the excitation function results we were led to the conclusion that E^* is independent of the target mass. This is a pronounced inconsistency and it is hard to see how more refined calculations of the cascade and evaporation steps can remove it. It may be that the cascade results which lead to fragmentation are so atypical that it is incorrect to compare results with the predictions of average prompt cascade calculations. Alternatively the production of such fragments as Na^{24} may go by a mechanism alien to the cascade-evaporation model.

It is noteworthy that the measurements imply a strong similarity in the average processes leading to Na^{24} or Mg^{28} production from all targets: excitation functions are almost proportional; the values of $v_{\parallel}$ and $E/E_{Coul.}$ are only slightly dependent on target mass for each incident energy. The prompt cascade calculations[5] lead one to expect much more variation in these quantities.

IV. FRAGMENTATION MECHANISMS

A. Experimental Findings Requiring Explanation

The difficulties and inconsistencies cited above lead us to abandon the cascade-evaporation description of the mechanism responsible for production of Na^{24} and Mg^{28}. Before we consider possible alternative mechanisms let us summarize some of the main features which an adequate reaction mechanism must explain.

(1) Fragment production is associated with high energy transfer to the target nucleus.

(2) Excitation functions rise steeply for bombarding energies up to about 1 GeV. Above this energy there is a pronounced leveling off in yield.

(3) The excitation functions for Na^{24} and Mg^{28} have the same shape whether protons or helium ions are used as bombarding particles, but the yields run a factor of approximately two higher when helium ions are used. This finding is one of the most important results of our experiments. We conclude that the cascade initiated by a high energy helium ion is remarkably similar to that initiated by a proton of the same energy.[‡] In the absence of detailed information on the elastic and inelastic scattering of high energy helium ions from single nucleons it is difficult to decide how to set up a Monte Carlo calculation for the interaction of a high energy helium ion with a complex nucleus. Without any experimental information to settle the point we think it unlikely that mesons would be produced in the same intensity and with the same yield-energy dependence when helium ions are substituted for protons. Hence we think that the meson production and reabsorption mechanism of fragmentation (discussed in Section B below) is not supported by our results.

(4) Na^{24} and Mg^{28} have very substantial recoil energies in all cases studied. These energies are roughly equal to that which they would receive

by Coulombic repulsion in a fission-like division of the target nucleus into two large pieces.

(5) The yield of these products goes through a minimum as a function of target atomic number as shown in Figs. 5 and 6.

(6) The ratio of the yield of Mg^{28} to that of Na^{24} is substantially less than 1 and for a given target remains remarkably constant when the helium ion energy is varied or when protons are substituted for helium ions as the bombarding particle. See Table I.

(7) If the light fragments observed in emulsion studies (represented chiefly by Li^{8}) are produced in the same type of events as those which produce Na^{24} or Mg^{28} then there is a whole series of their properties which must be accounted for. Among them we may mention such features as their anisotropic emission (strong forward peaking), their unexpectedly high rate of multiple emission, and the favoring of fragments of low excitation near the line of beta stability. These and other features are discussed fully in the review paper of Perfilov, Lozhkin and Shamov.[10]

With these features in mind let us examine various suggestions of the causes of fragmentation phenomena.

B. Suggested Mechanisms

A consideration of the differing radiochemical yields in targets of lead or bismuth bombarded with protons of various energies up to 3 GeV led Wolfgang et al.[24] to postulate that fragment production was the result of the creation of mesons and the reabsorption of these mesons before they could escape. Such a process would occur only above the meson production threshhold ($\approx$ 300 MeV) and would be most effective in the heavier elements. The reabsorption of a π-meson by a pair of nucleons would release two high energy

nucleons which would break numbers of neighboring nucleon-nucleon bonds and perhaps lead to a rapid cleavage of the nucleus.

This mechanism may contribute to the Na^{24} production which we observe, but there are several pieces of evidence which seem to us to argue against it as the only or even as the chief contributor. There is some yield of fragments even below the meson creation threshold. Furthermore we observed the unexpected result that Na^{24} and Mg^{28} yields are very similar when helium ions were substituted for protons of a given energy. This is contrary to what one would have expected on the meson-related hypothesis, since it is believed that helium ions should be less effective than protons of the same energy for the production of mesons. The pattern of reaction products in targets bombarded with a beam of π-mesons has been investigated[43] and it is not substantially different from that observed when protons are the bombarding particle; in particular, there is not a greatly increased yield of fragments. Russian studies of light fragment production in emulsions bombarded with positive pions of low and high energy show that fragments may indeed be produced by the absorption of pions; however, at the higher pion energies the elastic collisions of pions with protons in the nucleus may lead to fragment production even if the pions are not absorbed. Apparently what is certrally important is the buildup of a complex cascade.

Another suggestion is one made by Blokhintsev[44] and by others that the incoming particle makes an inelastic collision with clusters of nucleons, knocking the cluster out of the nucleus. This mechanism has been more commonly suggested to explain the production of light fragments like Li^8. But Sörensen[18] and others[11,14,17] have found that the angular distribution of such light fragments is not in agreement with this model; there are too many fragments ejected at large angles to the beam.

A highly original reaction mechanism was proposed by Glassgold, Heckrotte and Watson[45] who suggested that fragments are ejected from the nucleus by the action of shock waves originated by the "hole bored" by the passage of the bombarding particle through the nucleus. This model is not sufficiently developed so that detailed prediction of the products of the reaction can be quoted.

Lozhkin expresses his views on those interactions which lead to fragment production somewhat as follows.[46] Whenever a very complex cascade occurs in the initial phase of the reaction so that many fast nucleons appear in a relatively small volume of the nucleus within a short time ($\sim 10^{-22}$ seconds), normal nucleon-nucleon bonds cannot exist. Simultaneous with the development of the cascade the strong interactions between nucleons will cause local volume and surface distortions which will become increased by the interplay of surface tension and Coulombic repulsion forces. In this case there is high probability of individual nucleons or nucleon clusters breaking away from the nucleus if the directions of their momenta are suitable. The greater the energy liberated in the process of development of the cascade the greater the disturbance to the integrity of the nucleus and the greater the fragment yields. Lozhkin was primarily interested in the lighter fragments but undoubtedly the heavier fragments could be accounted for also by the splitting of the distorted nucleus under the Coulombic repulsion forces.

A somewhat similar view of high energy interactions has been expressed by Faissner and Schneider[47] to explain their emulsion studies of high energy fission. These authors examined fission tracks in emulsions loaded with a thorium compound which had been bombarded with 600 MeV protons. They selected fission events associated with high momentum transfer by a criterion based on deviations of the paths of the two fission fragments from 180°. They then

found that there was a forward-backward mass asymmetry associated with these high momentum events; the light fragment was preferentially ejected in the forward hemisphere. The mere existence of this fore-aft asymmetry proves that there must be a fast fission process which occurs almost simultaneously with the propagation of the nucleonic cascade. Faissner and Schneider[47] postulate that in those events in which many nucleons are struck in the development of the prompt cascade there occurs a conical flow of nuclear matter strongly localized along the direction of the beam. As this group of nucleons moves forward a viscous flow of nuclear matter occurs until a considerable portion of the nucleus is extended in the forward direction. This leads to a longitudinal deformation which may be sufficient to cause fission. The light fragment is ejected primarily in the forward direction because the cascade becomes sufficiently developed for such a deformation only after the initial proton and the cascade nucleons have penetrated well past the mid-point of the nucleus.

We agree with the essential features of these last two descriptions of the high energy fragmentation or fission process. In our own words we would express it as follows. The conventional model of a fast stage followed by a slow stage must be supplemented with a 2-stage process in which both stages are so rapid that there is no time for an equilibration of energy throughout the whole nucleus. In the first stage the essential feature is a very complex nucleonic cascade. Meson production with or without re-absorption may play a role but it does not play a unique role. The important point is that considerable kinetic energy is imparted to a large number of nucleons within a localized region along the direction of the incoming particles. Some of the light fragments may be formed from the many nucleons traveling together in the cascade. Two or more relatively cool regions of the nucleus

are separated by a group of fast moving nucleons. Viscosity effects cause further distortion of the nucleus and if these distortions are great enough, the Coulombic forces cause a rapid division of the nucleus into two or more parts.

We would also emphasize that the energetics of the distortion of the nucleus must play an important role. As a function of the charge and mass of the nucleus there are marked changes in the absolute amounts of energy required in particular types of distortion as well as marked changes in the favoring of certain types of distortions over others. These changes may have some bearing on the changes in yields and other properties of the products of a fission-like division of the nucleus as a function of the nuclear size. The best fundamental knowledge we have about these energetics are the potential-energy calculations of an ideal charged liquid drop made by Swiatecki and Cohen.[53] One of the important parameters in these calculations is the fissionability parameter x defined as the ratio $Z^2/A\ (Z^2/A)_{crit.}$ Z and A are the charge and mass number, respectively of the nucleus and $(Z^2/A)_{crit} = 50$ refers to a nucleus which is unstable toward fission for even the slightest distortion from the sphere. Swiatecki and Cohen have calculated the energy required to distort a nucleus with a given value of x into a variety of symmetric and unsymmetric shapes, particularly the energy required to form a drop of such shape (fission saddle shape) that no additional energy need be added to cause division into fragments.

These calculations show that the energy required to take a nucleus along a distortion path which leads ultimately to a division into equal fragments goes through a maximum in the middle of the system of elements (roughly at about mass 150). At low value of Z there is so little binding

energy in the nucleus that any conceivable distortion occurs with modest expenditure of energy. The heaviest elements require less energy to achieve a critical saddle shape distortion because of the great Coulombic energy of the protons in the incipient fragments. But stability toward asymmetric shape changes is also important. At the lower masses asymmetric shapes corresponding to the formation of a pear-shaped nucleus, and ultimately to the sucking up of one fragment by the other are strongly favored. As the value of the parameter x increases this holds true to a lesser extent until at a critical value of $x = 0.39$ the formation of a symmetric shape (a spheroid or a spheroid-like figure with a central waist) becomes favored. These two effects i.e. the passage of the deformation energy of the symmetric saddle point through a maximum and the favoring of symmetric over asymmetric distortion only at higher x values may have some bearing on the cross section curves of Figs. 5 and 6. If we speak of the Na^{24} produced by a fission-like process we may expect appreciable yields in the lightest targets just because of the low energy requirements for any sort of distortion and division of the nucleus. We expect a minimum in the medium weight elements because of the very high fission-barrier and partly because the potential energy of deformation favors pear-shaped over centrally-waisted figures. And, finally, the higher yields for high Z targets are expected owing to the low fission barriers.

Our argument is not that these static calculations of potential energies can provide any detailed explanation of fragmentation phenomena. We argue only that the big changes in the energetics must influence the outcome of any process in which the buildup of a distortion in the nucleus by a fast or a slow process is decisive in the final outcome. A complex nuclear cascade has the role of initiating a nuclear distortion. The

distortion which develops may be rather different in character from that which would develop in a nucleus excited to comparable energy by other processes. However, by our reasoning fragment formation could also be expected in nuclei excited to hundreds of MeV energy by other means.

APPENDICES

A. Radiochemical Procedures

The chemical procedures were adaptations of standard radiochemical methods.[48,49] The metal foils were dissolved with appropriate acids and the plastic foils destroyed with a hot mixture of sulfuric and nitric acids in the presence of 10 mg of Na carrier and 5 mg of Mg carrier. The sulfuric-nitric acid mixture was evaporated to dryness and the residue dissolved in distilled water. The target materials were removed by precipitation of copper sulfide, silver chloride or uranium tetroxide,[50] or, in the case of gold targets, by extraction of gold with ethyl acetate.

After this removal of the bulk of the target material the solution volume was adjusted to 10 ml. Iron hydroxide was precipitated once in the presence of ammonium chloride to scavenge out unwanted hydroxide-insoluble contaminants, and than copper, antimony, and nickel sulfides were precipitated. The excess hydrogen sulfide was removed and another precipitation of iron hydroxide was performed. Magnesium was precipitated with 8-hydroxyquinoline and the solution kept for sodium analysis. The magnesium hydroxyquinolate was destroyed. The hydroxide and sulfide precipitations were repeated. Calcium, strontium, and barium oxlates were twice precipitated and the final supernatant liquid was evaporated to dryness. The residue was taken up in water and strontium sulphate was precipitated (pH = 6). Iron hydroxide was precipitated once again and removed by filtration. Magnesium was precipitated with 8-hydroxyquinoline, filtered, dried at 110°C, weighed and mounted for counting.

The solution, containing the sodium fraction, was treated with a mixture of benzene and 1- butanol to remove excess hydroxyquinoline (and possibly quinolinates of impurities). The organic solution was discarded

and the aqueous solution was evaporated to dryness. The residue was dissolved in water. Sodium was precipitated as sodium magnesium uranyl acetate and converted to sodium chloride with hot 1-butanol saturated with dry HcL. This step was repeated. The sodium chloride precipitate was treated with concentrated perchloric acid, 5 mg of potassium chloride was added and the solution evaporated to dryness. Sodium perchlorate was extracted with 1-butanol and converted into sodium chloride with 1- butanol saturated with hydrogen chloride. The sodium chloride was filtered, dried at 110° weighed, and mounted. The chemical yield of Na^{24} or Mg^{28} was assumed equal to the percentage recovery of the 10 milligrams of inert sodium or 5 milligrams of magnesium added in the beginning.

The filtration apparatus has been described by Blann.[51] In part of this work glass filter pads were used to minimize weighing errors due to absorption of moisture.

B. Mounting of Samples and Determination of Their Radioactivity

Samples were mounted on aluminum plates (350 mg/cm^2) and covered with 0.1 mil pliofilm. The Na^{24} and Mg^{28} activity was measured by placing the sample in a reproducible geometry 0.9 cm from an end-window methane-flow proportional counter of 2.54 cm diameter. Measurements were repeated in a regular rotative sequence with a series of counters in order to minimize variations in efficiency and background. This rotation of samples was particularly important in the samples from the recoil catcher foils, particularly the backward catcher foils. Standard checks of counter performance were made daily.

The influence of sample thickness upon counting efficiency was determined by comparison of the counting rates of Na^{24} in a stack of aluminum

foils of different thicknesses bombarded with protons in a special irradiation. The relative counting efficiencies of Na^{24} and Mg^{28} was taken from Bayhurst and Prestwood.[52]

In the samples obtained from the recoil experiments it was necessary to evaluate error due to activation of impurities in the catcher foils. The Na^{24} produced in blank foils was always measurable and corresponded to a small percentage of the total Na^{24} activity found in the catchers. In the Mg^{28} experiments, on the other hand the activities were much lower and background activity due to activation was not measurable. However, since the activity of the Mg^{28} samples was very low, especially in the backward recoil catcher, activations of the order of 1 c/m could have introduced errors up to 10%.

In every Na^{24} sample there was a prominent 15 hour period which could easily be resolved from the background. Chemical yields were practically constant for all foils from a given experiment. The Mg^{28} activities were lower, the chemical yields somewhat variable, and the possible contribution from contaminants was higher. The uniformity in thickness of the copper, gold, and uranium targets was so high that there was negligible error from this source. Errors from thickness nonuniformity in the silver foils may have reached 5%. Errors caused by oxide film on the uranium are considered to be small. The overall error of the measurement (at the 95% confidence level) of the product, W x F, in the recoil experiments is considered to be of the order of 5% for Na^{24} produced in copper, gold, and uranium, and of the order of 10% in silver. The Mg^{28} errors are probably about twice as large.

C. Effects of Approximations Made in Calculating Ranges of Fragments and Velocities of Their Progenitors

(a) the effect of neglecting $\eta_\perp$

Eqs. (1), (2), and (3) given in the test can be rewritten in the following forms.

$$(7)\quad \frac{F_F}{F_B} = \frac{\left[1+\eta_\parallel \frac{2}{3}(N+2)+\eta_\parallel^2 \frac{(N+1)^2}{4}\right]+\eta_\perp^2 \frac{N^2-1}{8} + \frac{b}{a}\left[\frac{1}{6} + \eta_\parallel \frac{8(N-1)}{45} + \eta_\parallel^2 \frac{N^2-N-4}{12} + \eta_\perp^2 \frac{N-1}{12}\right]}{\left[1-\eta_\parallel \frac{2}{3}(N+2)+\eta_\parallel^2 \frac{(N+1)^2}{4}\right]+\eta_\perp^2 \frac{N^2-1}{8} + \frac{b}{a}\left[\frac{1}{6} - \eta_\parallel \frac{8(N-1)}{45} + \eta_\parallel^2 \frac{N^2-N-4}{12} + \eta_\perp^2 \frac{N-1}{12}\right]},$$

$$(8)\quad W(F_F - F_B) = R_o\, \eta_\parallel \left[\frac{N+2}{3} + \frac{b}{a}\frac{4(N-1)}{45}\right],$$

and

$$(9)\quad 4WF_P = R_{oP}\left[1 + \eta_\parallel^2 \frac{(N-1)(N+1)}{8}\right] + R_{oP}\left\{\eta_\perp^2 \frac{(N+1)(3N+1)}{16} + \frac{1}{6}\frac{b}{a}\left[-\frac{1}{2}+\eta_\perp^2 \frac{(7-3N)(N+1)}{16} + \eta_\parallel^2 \frac{(N-1)(N-5)}{8}\right]\right\}$$

It will be seen in Appendix IV that N takes the value 1.5 in Cu, Ag, Au, and U. In this case Eq. (7) becomes:

$$(10)\quad \frac{F_F}{F_B} = \frac{1+2.33\,\eta_\parallel + 1.56\,\eta_\parallel^2\left[1+0.1\,\eta_\perp^2/\eta_\parallel^2\right] + 0.04\,\frac{b}{a}\,\eta_\perp^2 + b/a(\ldots)}{1-2.33\,\eta_\parallel + 1.56\,\eta_\parallel^2\left[1+0.1\,\eta_\perp^2/\eta_\parallel^2\right] + 0.04\,\frac{b}{a}\,\eta_\perp^2 + b/a(\ldots)}$$

By inspection of Eq. 10 we decide that $\eta_\perp/\eta_\parallel$ must be much larger than 1 in order to introduce appreciable errors into the estimate of $\eta_\parallel$ if F_F/F_B is not extremely large. In order to get an estimate of the relative magnitudes of $\eta_\perp$ and $\eta_\parallel$ we refer to the information which Porile[42] extracted on this point by an examination of results of Monte Carlo calculations of the nucleon-nucleon cascade. He found that for large momentum transfers (such as are important in our experiments)

the ratio $\eta_\perp/\eta_\parallel$ is indeed much less than unity. Thus the neglect of $\eta_\perp$ is justified.

Since $R_o\ \eta_\parallel$ is independent of $\eta_\perp$ (Eq. 5), errors due to the neglect of $\eta_\perp$ are equally introduced in $\eta_\parallel$ and R_o. However $W(F_F - F_B) \propto R_o\ \eta_\parallel \propto V^{1/2}\ v_\parallel$ (for N = 1.5) and therefore $v_\parallel$ is practically independent of $\eta_\perp$.

(b) the effect of neglecting b/a

Possible effects of non-isotropic distribution of the products in the center-of-mass system of the progenitor are expressed by the term in b/a in Eq. 8 which for N = 1.5 reduces to

$$W(F_F - F_B) = k^{2/3}\ (1.16 + 0.044b/a)\ R_o^{1/3} v$$

For values of b/a smaller than 0.5 the influence of b/a on the expression enclosed in parentheses is negligible. The experimental data from WF_p and $W(F_F + F_B)$ measurements indicate that b/a is always less than 0.5. Thus the calculation of v is only affected through the influence of b/a on R_o.

D. Range Energy Relationships

The required range-energy relationships needed in our work for Na^{24} and Mg^{28} stopped in copper, silver, gold, and uranium were not available in the published literature and could not be easily obtained from theory. Consequently we derived the needed ralationships indirectly in the following way.

Heckman and co-workers[54] have measured the ranges in nuclear emulsions of nuclei of C, N, O, Ne, and A accelerated to energies of 0.5 to 10 MeV per atomic mass unit. They used the range, $\lambda(\beta)$, of a proton with velocity $\beta = v/c$ as their standard and discussed the observed ranges of the complex particles in terms of the corresponding range, $M/Z^2\ \lambda(\beta)$ (expected if no neutralization of charge occurred) and in terms of a range extension term, $R_{ext}(\beta)$, which corrected for the

pick-up of charge by the fragment as it loses energy. The range extension is defined by:

$$R_{ext}(\beta) = R(\beta) - \left(\frac{M}{Z^2}\right) \lambda(\beta)$$

where $R(\beta)$ is the observed range. Heckman et al.[53] found that a plot of $R_{ext}/MZ^{2/3}$ versus the velocity of the ions, expressed in units of the K-electron velocity, gave a universal curve. We evaluated the ranges of Na^{24} and Mg^{28} in emulsion by use of this universal curve and the above relation. In the energy interval 0.4 to 3.0 MeV/amu, the ranges are given by $R = 0.95\ (E/A)^{0.94}$, expressed in mg/cm^2. This range-energy relationship should be fairly accurate, since in this same energy interval the ranges of all complex particles are, for a given speed, the same within 20 percent.

The relative stopping powers of the nuclear emulsions and the target materials used in this work, for ions of a given speed, were determined by the ratios of the ranges of α particles or protons of the same velocity in nuclear emulsions and in the target material. This procedure is not absolutely correct, but it is a reasonable approximation. The ranges in emulsion of α particles and protons were taken from Barkas et al.[55] and Heckman et al.[54], respectively. The ranges of α particles and protons in Cu, Ag, and Au have been taken from Whaling.[56] The ranges of the fragments in uranium were assumed equal to the ranges of the fragments in gold. While there is published evidence[57-59] that this assumption is not strictly correct, the errors introduced by this assumption in the calculated recoil energies of the fragments produced in uranium should not exceed 10%. The range-energy relationships obtained for both Na^{24} and Mg^{28} are of the form $R = k\ (E/A)^{0.76}$ where k is a constant. With R expressed in mg/cm^2 and E/A in MeV/amu, the constant k takes the values of 4.5 for Cu, 5.8 for Ag and 8.1 for Au and U.

Table I. Formation cross sections (in mb) of Na^{24} and Mg^{28} from various target elements

		Alphas				Protons	
		320 MeV α	500 MeV α	700 MeV α	880 MeV α	700 MeV p	5.7 GeV p
Cu	σ Na^{24}	8.26×10^{-2}(1)	$2.80\pm0.13\times10^{-1}$(3)	$6.98\pm0.13\times10^{-1}$(3)	1.38 ± 0.57 (3)	3.68×10^{-1}(1)	
	σ Mg^{28}	1.15×10^{-2}(1)	0.37×10^{-1}(1)	0.91×10^{-1}(1)	0.19 (2)	0.49×10^{-1}(1)	
	σ $\frac{Mg^{28}}{Na^{24}}$	0.14	0.13	0.13	0.13	0.12	
	$\frac{Na^{24}}{Na^{22}}$					7.44[a]	1.65[b]
Ag	σ Na^{24}	3.25×10^{-2}(1)	$9.52\pm0.72\times10^{-2}$(3)	$2.27\pm0.005\times10^{-1}$(3)	$4.46\pm0.02\times10^{-1}$(3)	1.00×10^{-1}(1)	
	σ Mg^{28}	0.39×10^{-2}(1)	1.10×10^{-2}(1)	0.26×10^{-1}(1)	0.49×10^{-1}(2)	0.12×10^{-1}(1)	
	σ $\frac{Mg^{28}}{Na^{24}}$	0.12	0.12	0.12	0.11	0.12	
Au	σ Na^{24}	3.23×10^{-2}(1)	$10.68\pm0.28\times10^{-2}$(3)	$3.08\pm0.87\times10^{-1}$(3)	$5.94\pm0.16\times10^{-1}$(3)	1.35×10^{-1}(1)	
	σ Mg^{28}	2.07×10^{-2}(1)	6.24×10^{-2}(1)	1.02×10^{-1}(1)	1.98×10^{-1}(2)	0.54×10^{-1}(1)	
	σ $\frac{Mg^{28}}{Na^{24}}$	0.64	0.58	0.33	0.33	0.23	
	σ $\frac{Na^{24}}{Na^{22}}$						5.29

(Cont)

Table I (Continued)

		Alphas				Protons	
		320 MeV α	500 MeV α	700 MeV α	880 MeV α	700 MeV p	5.7 GeV p
	σ Na^{24}	9.41×10^{-2}(1)	$21.02 \pm 1.38 \times 10^{-2}$(2)	$5.02 \pm 0.05 \times 10^{-1}$(2)	$8.75 \pm 0.25 \times 10^{-1}$(3)	2.30×10^{-1}(1)	
	σ Mg^{28}	6.42×10^{-2}(1)	12.29×10^{-2}(1)	2.38×10^{-1}(1)	4.50×10^{-1}(2)	1.15×10^{-1}(1)	
U	$\sigma \frac{Mg^{28}}{Na^{24}}$	0.68	0.58	0.47	0.51	0.32	
	$\sigma \frac{Na^{24}}{Na^{22}}$						5.00[c]

[a]Reference 35.

[b]From D. W. Barr, report UCRL-3793, 1957, unpublished.

[c]From C. L. Carnahaw, report UCRL-8026, 1957, unpublished.

Table II. Comparison of yields of Na^{24} (and Mg^{28}) in targets bombarded with 700-MeV protons and helium ions.

Target	$\frac{\text{Yield } Na^{24} \text{ (700-MeV He)}}{\text{Yield } Na^{24} \text{ (700-MeV p)}}$	$\frac{\text{Yield } Mg^{28} \text{ (700-MeV He)}}{\text{Yield } Mg^{28} \text{ (700-MeV p)}}$
Cu	1.9	1.85
Ag	2.27	2.17
Au	2.28	1.85
U	2.18	2.07

Table III. Summary of Na^{24} recoil results from the forward-backward experiments

1	2	3	4	5	6	7	8	9	10	11	12
Tgt.	No.	Beam	$W F_F$ (mg/cm^2)	$W F_B$ (mg/cm^2)	F_F/F_B	η	R_o (mg/cm^2)	E (MeV)	v (MeV/amu)$^{1/2}$	$\bar{P}_T$ (amu MeV)$^{1/2}$	$\bar{P}_T/P_{CN}$
	2	880 MeV α	1.678±0.055	0.202±0.000	8.23±0.29	0.42	2.99	14.4	0.46	29.4	0.33
	1	700 MeV p	1.184	0.352	3.37	0.25	2.81	13.2	0.27	16.9	0.38
Cu	1	3 GeV p	1.036	0.370	2.79	0.22	2.63	12.1	0.22	13.8	0.10
	1	320 MeV α	(2.440)	(0.338)	(7.19)						
	2	880 MeV α	3.345±0.072	0.645±0.002	5.09±0.13	0.33	6.88	30.2	0.53	57.3	0.64
	1	700 MeV p	2.253	0.969	2.32	0.18	6.18	25.7	0.26	28.1	0.63
Ag	1	3 GeV p	1.848	0.813	2.27	0.17	5.10	20.4	0.23	24.4	0.21
	3	880 MeV α	6.576±0.096	2.166±0.072	3.03±0.06	0.23	16.22	60.0	0.52	102.6	1.15
	1	700 MeV p	4.728	2.796	1.68	0.11	14.92	54.0	0.23	46.4	1.05
Au	1	3 GeV p	4.560	2.184	2.09	0.16	13.05	45.6	0.30	59.9	0.52
	1	6.2,4.5 GeV p	4.452	2.202	2.01						
	1	320 MeV α	(5.370)	(2.718)	(2.01)						
	5	880 MeV α	6.200±0.035	2.230±0.024	2.77±0.03	0.21	15.82	58.1	0.47	112.6	1.26
U	3	700 MeV p	4.165±0.081	2.520±0.043	1.64±0.006	0.106	13.30	46.1	0.21	49.3	1.12
	1	3 GeV p	5.450	2.635	2.06	0.15	15.66	56.6	0.33	79.5	0.68

-41-

UCRL-10496

Table IV. Summary of Na^{24} recoil results from the perpendicular experiments.

1	2	3	4	5	6	7
Target	Number of Determ.	Bombarding particle and its energy	$W F_{PF}$ (mg/cm^2)	$W F_{PB}$ (mg/cm^2)	R_{oP} (mg/cm^2)	R_o/R_{oP}
Cu	1	880 MeV α	0.818	0.642	2.84	1.05
	1	700 MeV p	0.664	0.630	2.56	1.10
	1	3 GeV p	0.742	0.576	2.62	1.00
Ag	1	880 MeV α	1.866	1.494	6.60	1.04
	1	700 MeV p	1.506	1.443	5.86	1.05
	1	3 GeV p	1.335	1.155	4.95	1.03
Au	1	880 MeV α	4.218	3.498	15.30	1.06
	1	700 MeV p	3.816	3.720	15.04	0.99
	1	3 GeV p	3.702	3.198	13.73	0.95
U	2	880 MeV α	4.025 ±0.001	3.285 ±0.169	14.51	1.09
	1	700 MeV p	3.340	3.235	13.11	1.01
	1	3 GeV p	4.140	3.515	15.24	1.03

Table V. Summary of Mg^{28} recoil results from the forward-backward experiments

1	2	3	4	5	6	7	8	9	10	11	12
Tgt.	No.	Beam	$W F_F$ (mg/cm^2)	$W F_B$ (mg/cm^2)	F_F/F_B	η	R_o (mg/cm^2)	E (MeV)	v (MeV/amu)$^{1/2}$	$\bar{P}_T$ (amu MeV)$^{1/2}$	$\bar{P}_T/P_{CN}$
	2	880 MeV α	1.546 ±0.013	0.176 ±0.011	8.80 ±0.66	0.43	2.70	14.5	0.44	28.2	0.31
Cu	1	700 MeV p	1.122	0.272	4.13	0.29	2.47	13.1	0.29	18.2	0.41
	1	3 GeV p	0.990	0.328	3.02	0.23	2.44	12.9	0.22	14.2	0.12
	2	880 MeV α	3.042 ±0.050	0.669 ±0.014	4.54 ±0.03	0.31	6.50	32.7	0.48	51.6	0.58
Ag	1	700 MeV p	1.995	0.897	2.22	0.17	5.53	26.6	0.23	25.3	0.57
	1	3 GeV p	1.749	0.801	2.18	0.16	4.92	22.9	0.21	22.8	0.19
	3	880 MeV α	6.744 ±0.221	2.520 ±0.041	2.67 ±0.07	0.21	17.49	77.0	0.48	95.6	1.07
Au	1	700 MeV p	5.484	3.570	1.53	0.09	18.02	80.3	0.22	42.9	0.97
	1	3 GeV p	5.160	2.514	2.05	0.15	14.92	63.0	0.32	63.5	0.54
	2	880 MeV α	7.420	3.085	2.46	0.19	19.55	89.6	0.48	114.3	1.27
U	1	700 MeV p	5.320	3.330	1.52	0.09	18.94	85.4	0.22	52.9	1.20
	1	3 GeV p	5.870	3.145	1.86	0.13	17.69	78.4	0.31	74.3	0.64

-43-

UCRL-10496

Table VI. Summary of Mg^{28} recoil results from the perpendicular experiments.

1 Target	2 Number of Determ.	3 Bombarding particle and its energy	4 $W F_{PF}$ (mg/cm^2)	5 $W F_{PB}$ (mg/cm^2)	6 R_{oP} (mg/cm^2)	7 R_o/R_{oP}
Cu	1	3 GeV p	0.688	0.538	2.43	1.00
Au	1	880 MeV α	4.932	3.684	17.12	1.02
	1	700 MeV p	4.842	4.644	18.95	0.95
	1	3 GeV p	4.236	3.816	16.04	0.93
U	1	880 MeV α	4.080	3.710	15.5	1.26
	1	3 GeV p	4.800	4.290	18.1	0.98

FOOTNOTES AND REFERENCES

* This report is a revision of the material published in the Ph.D. thesis of one of us V. P. Crespo, previously issued as Lawrence Radiation Laboratory Report UCRL-9683 Sept. 6, 1961.

† Present address, University of Coimbra, Coimbra Portugal.

‡ Additional evidence in support of this point comes from an unpublished study by Korteling and Hyde in which the excitation functions of a variety of products were studied in the interaction of high energy protons and helium ions with niobium targets over the bombarding energy range 240-880 MeV. The results of the proton-induced reactions were remarkably similar to those for helium-ion-induced reactions.

1. M. L. Goldberger, Phys. Rev. 74, 1269 (1948).
2. J. Combe, Nuovo Cimento 3, 182 (1956).
3. J. W. Meadows, Phys. Rev. 98, 744 (1955).
4. G. Rudstam, Thesis, Uppsala (1956).
5. Metropolis, Bivens, Storm, Turkevich, Miller, and Friedlander, Phys. Rev. 110, 185 (1958); 110, 204 (1958).
6. I. Dostrovsky, P. Rabinowitz, and R. Bivens, Phys. Rev. 111, 1659 (1958); I. Dostrovsky, Z. Fraenkel, and P. Rabinowitz, Proceedings of the Second United Nations International Conference on the Peaceful Uses of Atomic Energy, United Nations, Geneva 1958, Vol. 15, p. 301.
7. G. Friedlander, Z. Fraenkel, and I. Dostrovsky, Phys. Rev. 116, 683 (1959). J. Hudis and J. M. Miller, Phys. Rev. 112, 1322 (1958).
8. I. Dostrovsky, Z. Fraenkel, and J. Hudis, Phys. Rev. 123, 1452 (1961) I. Dostrovsky, Z. Fraenkel, and P. Rabinowitz, Phys. Rev. 118, 791 (1960).
9. J. M. Miller and J. Hudis, Ann. Rev. Nucl. Science 9, 159 (1959).

10. N. A. Perfilov, O. V. Lozhkin, and V. P. Shamov, Soviet Physics Uspekhi, 3 (60) 1-174, 1960.

11. O. V. Lozhkin and N. A. Perfilov, Sov. Phys. JETP 4, 790 (1957).

12. V. S. Ostroumov and Iu.P. Yakovlev, Sov. Phys. JETP 8, 949 (1959).

13. O. Skjeggestad and S. O. Sörensen, Phys. Rev. 113, 1115 (1959).

13a. P. A. Goritchev et al., Phys. Rev 126, 2196 (1962).

14. B. A. Munir, Phil. Mag. [8] 1, 355 (1956).

15. S. Katcoff, Phys. Rev. 114, 905 (1959).

16. D. H. Perkins, Proc. Roy. Soc. (London) 203, 399 (1950).

17. S. Nakagawa, E. Tamai, and S. Namoto, Nuovo Cimento [10] 9, 780 (1958).

18. S. O. Sörensen, Phil. Mag. 40, 947 (1949); ibid 42, 188, (1951).

19. E. W. Baker and S. Katcoff, Phys. Rev. 123 641 (1961).

20. Goldsack, Lock, and Munir, Phil. Mag. 2, 149 (1957).

21. Pickup and Voyvodic, Can. J. Research 28A, 616 (1950).

22. F. S. Rowland and R. L. Wolfgang, Phys. Rev. 110, 175 (1958).

23. E. Baker, G. Friedlander, and J. Hudis, Phys. Rev. 112, 1319 (1958).

24. R. Wolfgang, E. W. Baker, A. A. Caretto, J. B. Cumming, G. Friedlander, and J. Hudis, Phys. Rev. 103, 394 (1956).

24a. G. Friedlander and L. Yaffe Phys. Rev. 117, 578 (1960).

25. A. A. Caretto, J. Hudis, and G. Friedlander, Phys. Rev. 110, 1130 (1958).

26. A. K. Lavrukhina, L. P. Moskaleva, L. D. Krasavina, and I. M. Grechishcheva, Soviet J. Atom Energy 3, 1087 (1957).

27. J. B. Cumming, G. Friedlander, and C. E. Swartz, Phys. Rev. 111, 1386 (1958); R. L. Wolfgang and G. Friedlander, Phys. Rev. 96, 190 (1954); 98 1871 (1955); N. Horwitz and J. J. Murray, Phys. Rev. 117, 1361 (1960); P. A. Benioff, Phys. Rev. 119, 316 (1960).

28. M. Lindner and R. Osborne, Phys. Rev. 91, 342, (1953).

29. W. E. Crandall, G. P. Millburn, R. V. Pyle and W. Birnbaum, Phys. Rev. 101, 329 (1956).

30. R. E. Batzel, D. R. Miller, and G. T. Seaborg, Phys. Rev. 84, 671 (1951).

31. D. H. Greenberg and J. M. Miller, Phys. Rev. 84, 845 (1951).

32. A. P. Vinogradov, et al., Conference of the Academy of Sciences of the USSR on the Peaceful Use of Atomic Energy, July 1-5 (1955).

33. P. K. Kofstad, University of California Lawrence Radiation Laboratory Report, UCRL 2265, June (1953) unpublished.

34. B. V. Kurchatov et al., Proceedings of the Conference of the Academy of Sciences of the USSR on the Peaceful Use of Atomic Energy, Session on Chemical Sciences, July 1-5, 1955.

35. A. P. Vinogradov et al., loc cit ref. 34.

36. R. L. Folger, P. C. Stevenson, and G. T. Seaborg, Phys. Rev. 98, 107 (1955).

37. N. A. Perilov, N. S. Ivanova, O. V. Lozhkin, M. M. Makarov, I. V. Ostroumov, Z. I. Solovéua and V. P. Shamov, J. Exptl. Theor. Phys. (USSR) 38, 345 (1960) (translation: Soviet Phys. JETP 11, 250 (1960).

38. N. T. Porile and N. Sugarman, Phys. Rev. 107, 1422 (1957).

39. N. Sugarman, M. Campos, and K. Wielgoz, Phys. Rev. 101, 388 (1956).

40. N. Sugarman, private communication; N. Sugarman and J. Panontin, to be published.

41. L. Winsberg, University of California Lawrence Radiation Laboratory Report, UCRL 8618, pp. 44-52, 1959 unpublished.

42. N. Porile, Phys. Rev. 120, 572 (1960).

43. Ivanova, Sov. Phys. JETP 7, 955 (1958).

44. D. I. Blokhintsev, Sov. Phys. JETP 6, 955 (1958).

45. A. E. Glassgold, W. Heckrotte and K. M. Watson, Ann. Phys. 6, 1 (1959).

46. O. V. Lozhkin as reported reference 10.

47. H. Faissner and H. Schneider, Nuclear Physics 19, 346 (1960) and unpublished results presented at the CERN Conference on Fission and Spallation Phenomena and their Application to Cosmic Rays, Sept. 26-29, 1961.

48. J. R. Grover, Phys. Rev. 126, 1540 (1962).

49. Los Alamos Scientific Laboratory Report, LA-1721, Dec. 1954, unpublished.

50. Analytical Chemistry of the Manhattan Project, McGraw Hill Book Co., New York, 1950, p. 48.

51. H. M. Blann, University of California, Lawrence Radiation Laboratory Report UCRL-9190, May 1960, unpublished.

52. B. P. Bayhurst and R. J. Prestwood, Nucleonics 17, 82 (1959).

53. S. Cohen and W. J. Swiatecki "The Deformation Energy of a Charged Drop" Aarhus University report, Aarhus, Denmark January 1961 and later unpublished calculations.

54. H. H. Heckman, B. L. Perkins, W. G. Simon, F. M. Smith, and W. H. Barkas, Phys. Rev. 117, 544 (1960).

55. W. H. Barkas, P. H. Barret, P. Cüer, H. Heckman, F. M. Smith, and H. K. Tiche, Nuovo cimento 8, 185 (1958).

56. W. Whaling in Handbuch der Physik edited by S. Flügge (Springer-Verlag, Berlin 1958), Vol. 34, p. 193.

57. J. B. Niday, Phys. Rev. 121, 1471 (1961).

58. J. M. Alexander and M. F. Gazdik, Phys. Rev. 120, 874 (1960).

59. Garin and Faraggi, J. Phys. Radium 19, 76 (1958).

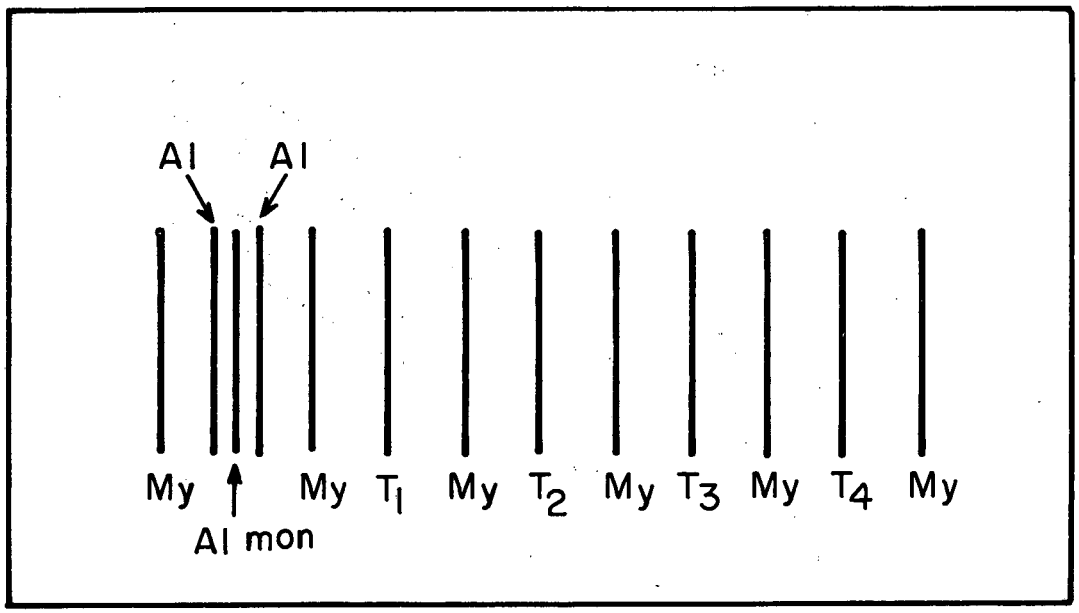

MU-24559

Fig. 1. The cross-section assembly. T_1, T_2, T_3, and T_4 are the target foils separated by 0.003-in.- thick Mylar spacers (My); Al_{mon} is the Al monitor foil. The other Al foils are guard foils.

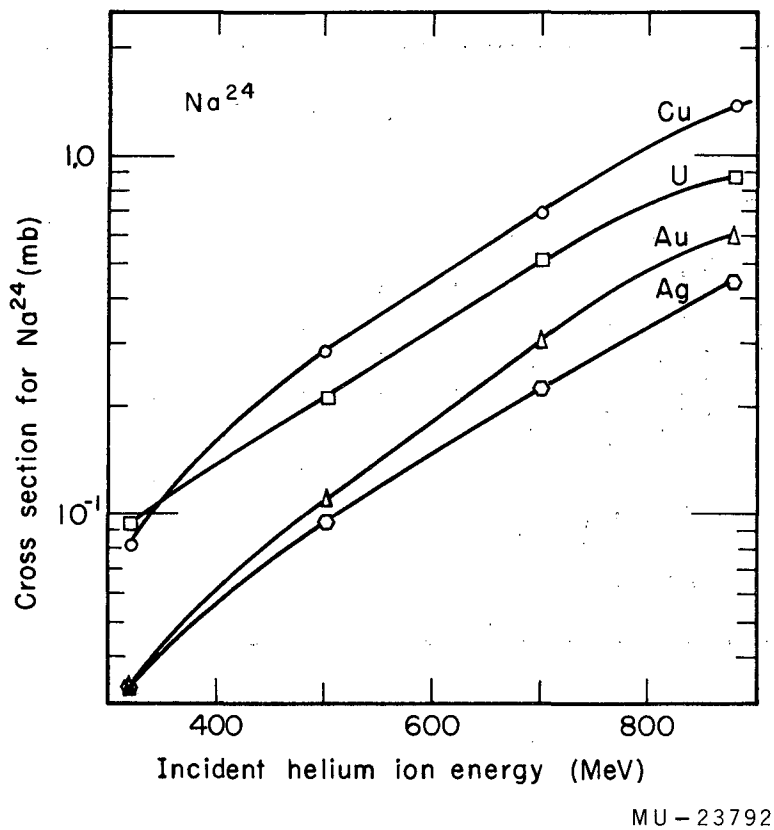

Fig. 2. Excitation functions for the production of Na^{24} from He ion bombardments of Cu, Ag, Au, and U.

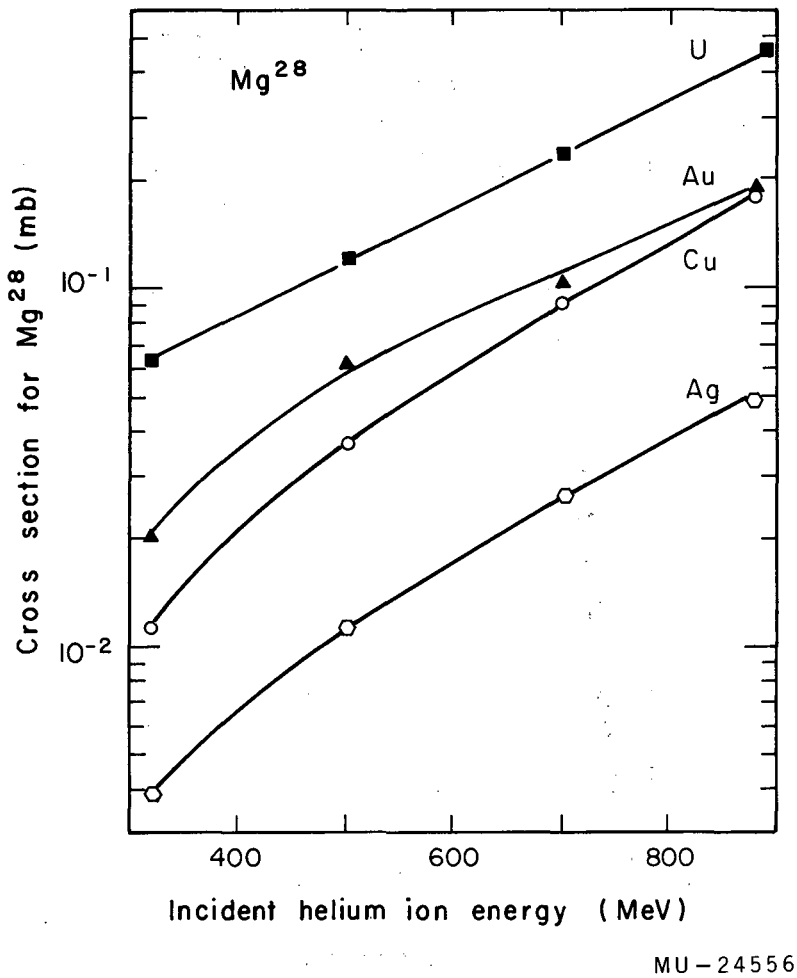

Fig. 3. Excitation functions for the production of Mg^{28} from He ion bombardments of Cu, Ag, Au, and U.

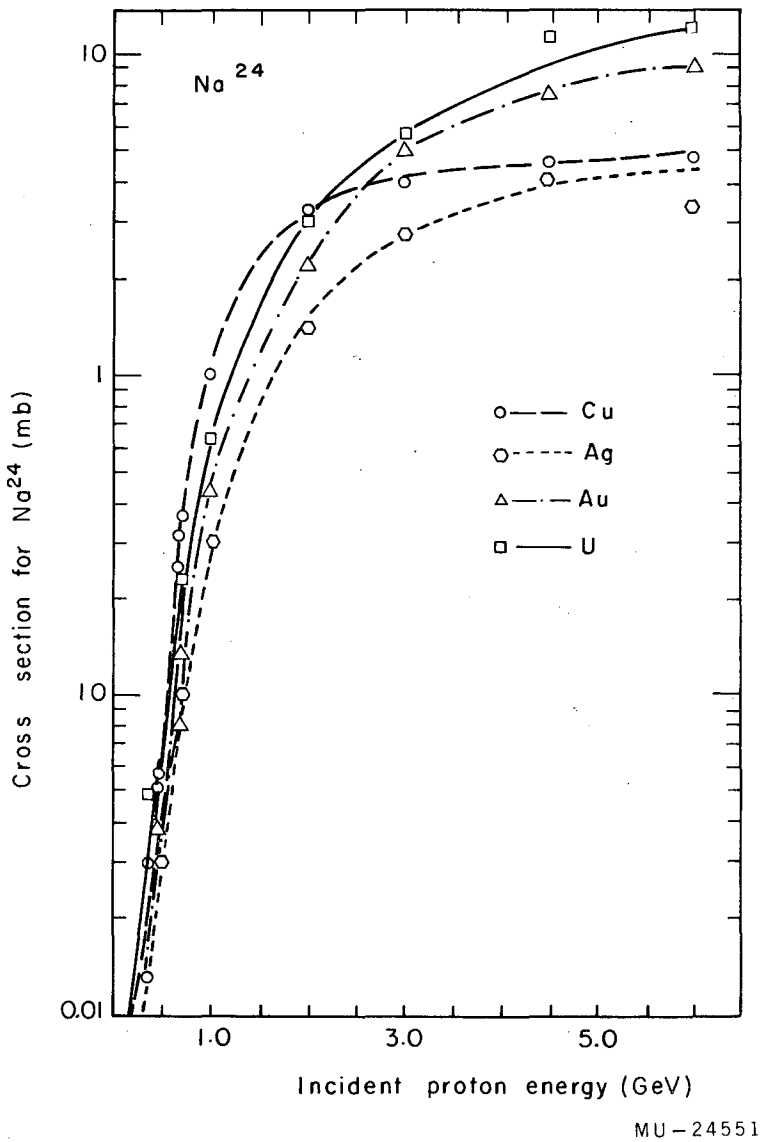

Fig. 4. Excitation functions for the production of Na^{24} from proton bombardments of Cu, Ag, Au, and U. Data from 1 to 5.9 GeV from Ref. 25. Data for Cu are from Refs. 31, 32, 30, 26, for Ag from Refs. 33 and 34, for Au from Ref. 26 and for U from Refs. 35 and 36. The 700-MeV points are from this work.

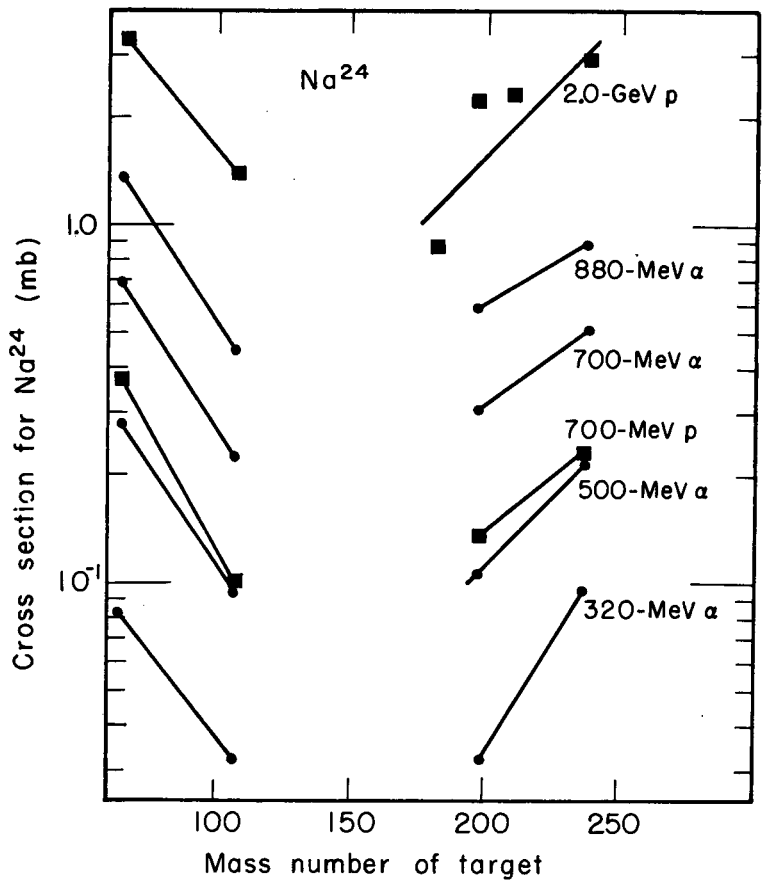

MU-23797

Fig. 5. Formation cross section of Na^{24} vs target mass number. The points on the 2 GeV p curve are taken from Ref. 25.

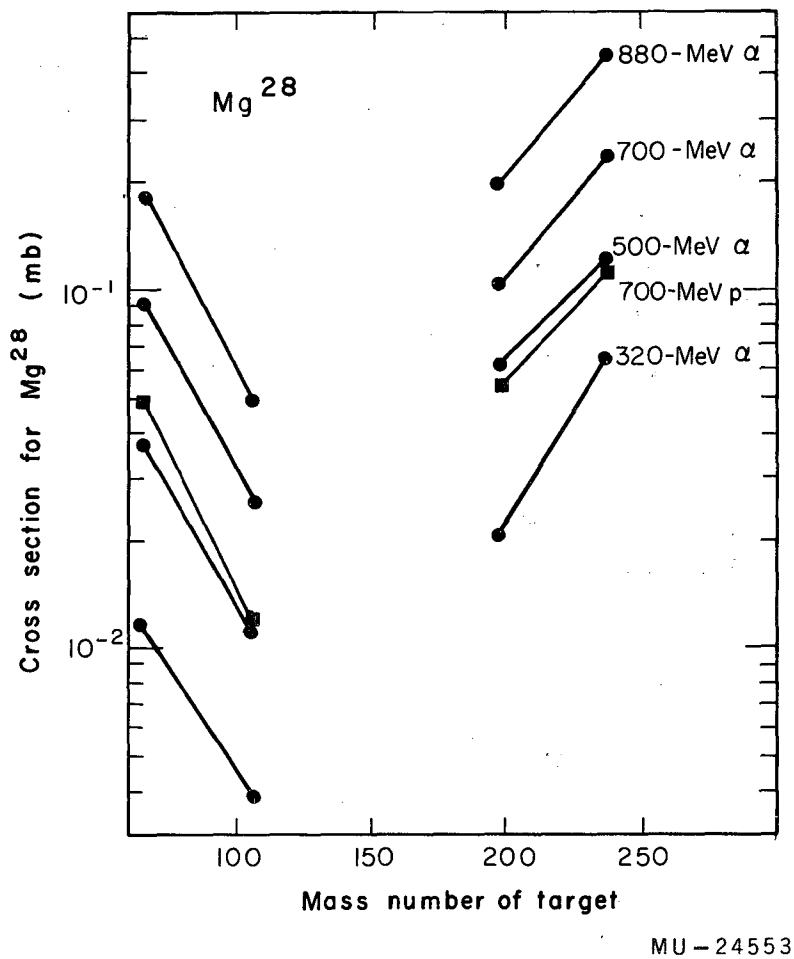

Fig. 6. Formation cross section of Mg^{28} vs target mass number.

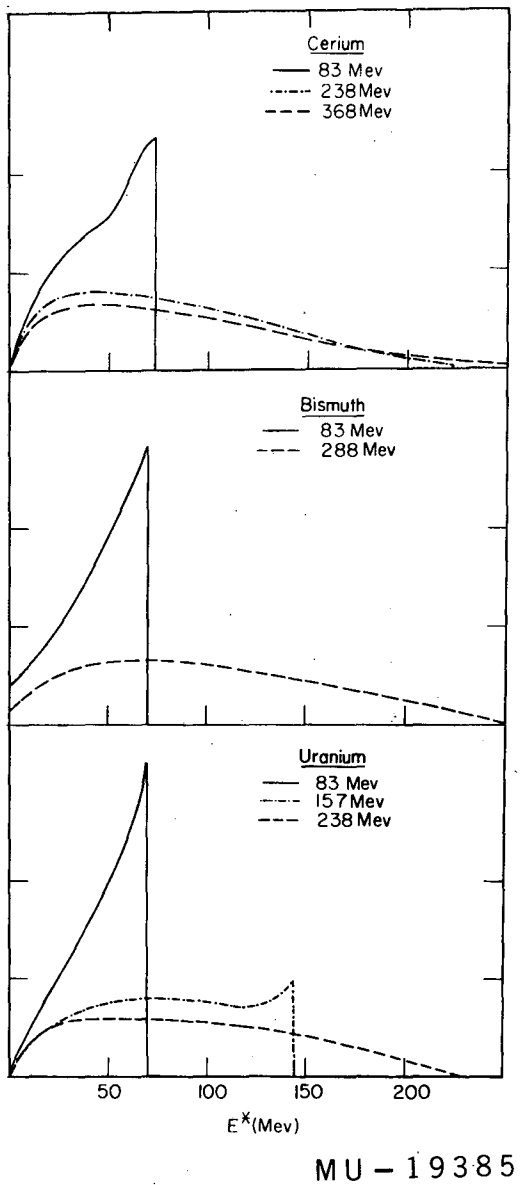

Fig. 7. Gross distribution of excitation energies $N(E^*)$ calculated by Metropolis et al.[5] for bombardments of cerium target with 238 and 368 MeV protons.

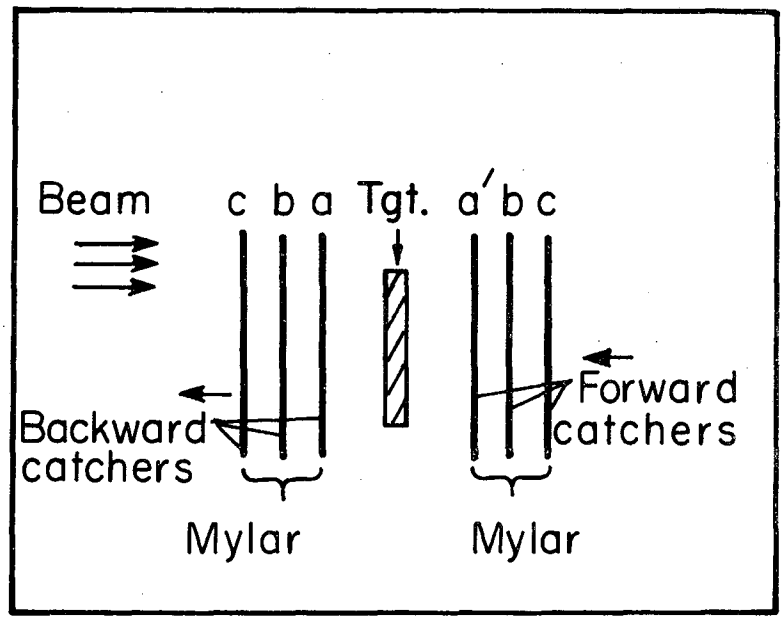

MU-24554

Fig. 8. The recoil assembly. The recoils generated in the target foil T were caught in the catcher foils a and a'. Foils b were used as blank foils; foils c were guard foils. All the catcher foils were 0.003-in.-thick Mylar.

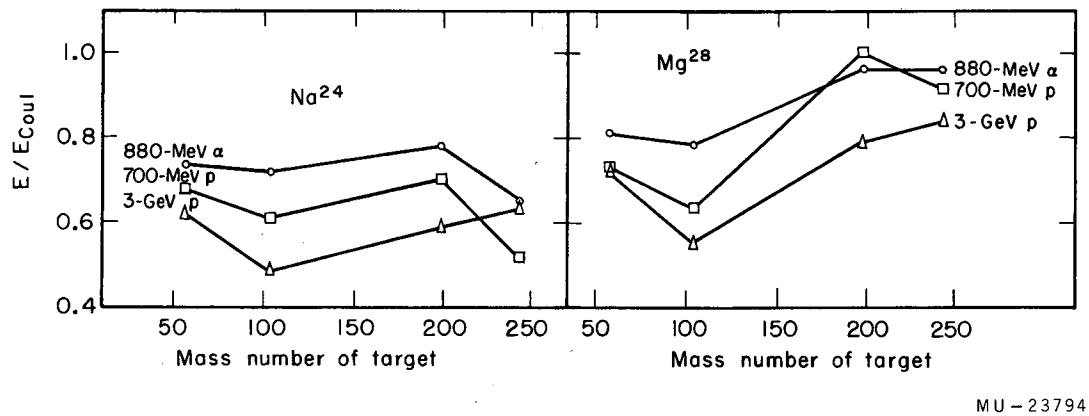

Fig. 9. Ratio for Na^{24} and Mg^{28} of the intrinsic recoil energy to the Coulomb energy (see text) as a function of the target mass.

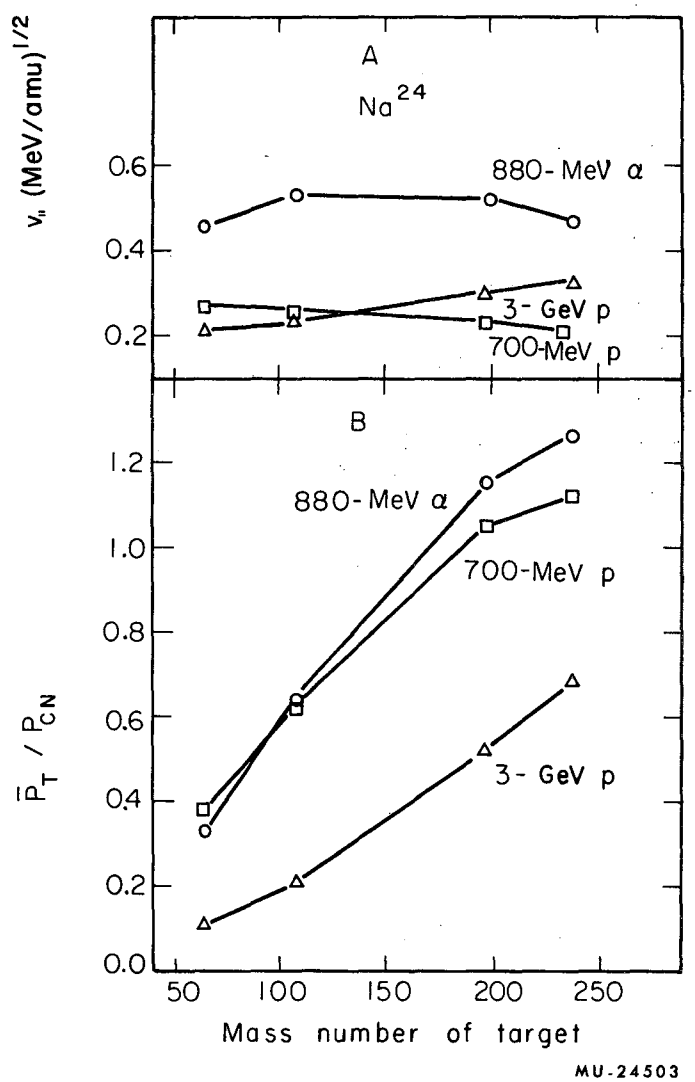

Fig. 10. Imparted velocity $v_{\parallel}$ (A) and fractional imparted momentum $\bar{P}_T/P_{CN}$ (B) for Na^{24} as a function of the target mass.

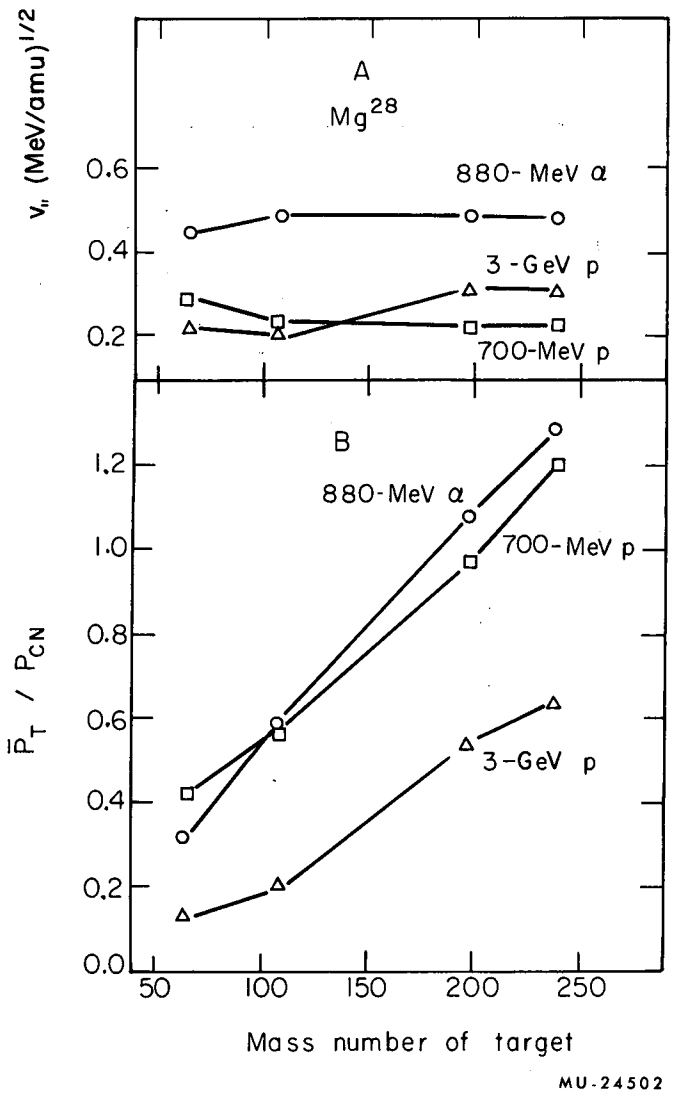

Fig. 11. Imparted velocity $v_{\parallel}$ (A) and fractional imparted momentum $\bar{P}_T/P_{CN}$ (B) for Mg^{28} as a function of target mass.

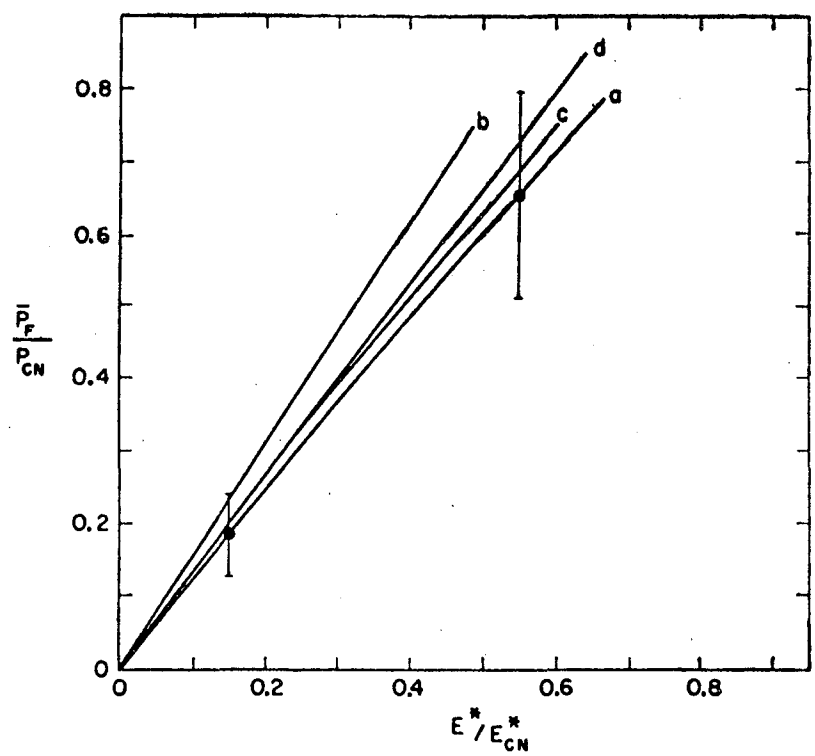

MU-23688

Fig. 12. Variation of the average forward momentum with excitation energy. a: U or Bi, 0.46 GeV; b: Bi, 0.94 GeV; c: Bi, 1.84 GeV; d: Ru, 0.46 GeV (after Porile, Ref. 42).

This report was prepared as an account of Government sponsored work. Neither the United States, nor the Commission, nor any person acting on behalf of the Commission:

A. Makes any warranty or representation, expressed or implied, with respect to the accuracy, completeness, or usefulness of the information contained in this report, or that the use of any information, apparatus, method, or process disclosed in this report may not infringe privately owned rights; or

B. Assumes any liabilities with respect to the use of, or for damages resulting from the use of any information, apparatus, method, or process disclosed in this report.

As used in the above, "person acting on behalf of the Commission" includes any employee or contractor of the Commission, or employee of such contractor, to the extent that such employee or contractor of the Commission, or employee of such contractor prepares, disseminates, or provides access to, any information pursuant to his employment or contract with the Commission, or his employment with such contractor.